CSIRO
AUSTRALIA

EXPLORATION
AND MINING

EXPLORATION AND MINING REPORT 181C

PETROPHYSICAL CHARACTERISATION OF MAGNETITE CONCENTRATES

P.W. Schmidt and D.A. Clark

CSIRO
AUSTRALIA

DIVISION OF EXPLORATION AND MINING
Institute of Minerals, Energy and Construction

EXPLORATION AND MINING REPORT 181C

PETROPHYSICAL CHARACTERISATION OF MAGNETITE CONCENTRATES

P.W. Schmidt and D.A. Clark

Prepared for BHP Australia Coal Pty. Ltd.

October 1995

COMMERCIAL-IN-CONFIDENCE

CSIRO Division of Exploration and Mining
PO Box 136, North Ryde, NSW, Australia 2113

Distribution List

	Copy No.
R.B. Kitch and BHP	1-3
B.E. Hobbs, Chief, CSIRO Exploration and Mining	4
P.W. Schmidt, CSIRO Exploration and Mining	5
D.A. Clark, CSIRO Exploration and Mining	6
Records Section (North Ryde)	7

Copy No. ....5.... of 7 copies

Summary

Petrophysical measurements have been performed on 24 magnetite concentrates supplied by Mr R.B. Kitch on behalf of BHPCA. The properties measured were (low field) magnetic susceptibility and its variation with temperature (k-T), hysteresis parameters including coercivity, saturation magnetisation and saturation remanence, and density. In addition, hysteresis parameters from two extra samples from the Rock Magnetism Laboratory collection of well characterised magnetite deposits, Savage River Mine, Tasmania, and Tasu Mine, British Columbia, have been included in the report for comparison.

Plots of saturation magnetisation versus susceptibility, saturation magnetisation versus density, saturation magnetisation versus coercivity and coercivity versus susceptibility show systematic trends with high correlation coefficients. The first two relationships are positive while the latter two are negative.

Of all the samples two outliers are apparent. Good correlations between saturation magnetisation and coercivity on the one hand, and coercivity and susceptibility on the other hand, were achieved only after omitting the Trevorite sample, which possesses an anomalously high coercivity (>200 Oe) and sample KO-02 which has an anomalously low coercivity for its (low) saturation magnetisation and susceptibility. These latter quantities are negatively correlated with coercivity. The former sample is highly doped with nickel, which is reflected in its k-T curve, and may not be expected to fall on the magnetite trend. The latter sample is soft MD magnetite from its k-T curve, although it is very diluted giving low saturation magnetistion and susceptibility. Another sample which displays an interesting k-T curve is the sample of fly-ash which may be heavily doped with aluminium. Doping magnetite with cations of Ti, Ni and Al reduces the Curie temperature which is clearly reflected in the k-T curves.

Properties of known magnetites used for Heavy Medium Separation (HMS) consistently plot close to the extremes of each relationship. The three HMS magnetites, Biggenden, Savage River and Tasu, have a mean coercivity of 46 Oe, a mean (specific) saturation magnetisation of 86 emu/g, and a mean (mass) susceptibility of 0.025125 emu/g. The relationship of saturation magnetisation versus susceptibility appears to be the best discriminator between pure magnetite and other compositions.

1. Introduction

As part of BHPAC's magnetite project, petrophysical measurements have been performed on a total of 24 magnetite concentrates supplied by Mr R.B. Kitch. The properties measured were (low field) magnetic susceptibility and its variation with temperature (k-T), hysteresis parameters including coercivity, saturation magnetisation and saturation remanence, and density. In addition, hysteresis parameters from two extra samples from the Rock Magnetism Laboratory collection of well characterised magnetite deposits, Savage River Mine, Tasmania, and Tasu Mine, British Columbia, have been included in the report for comparison.

2. Hysteresis, Susceptibility and Density

Hysteresis measurements were performed using an ARUN device which has been extensively modified in-house and interfaced to a PC. A "saturation" field of about 2000 Oe was used. Low field (~7 Oe) susceptibilty and its variation with temperature was measured using an in-house transformer bridge interfaced to a PC. Densities were measured by weighing samples dry and immersed in ethanol using a Mettler balance.

The petrophysical properties are listed in Table 1, while hysteresis plots are given in the appendix. Plots of saturation magnetisation versus susceptibility, saturation magnetisation versus density, saturation magnetisation versus coercivity and coercivity versus susceptibility show systematic trends with high correlation coefficients. The first two relationships are positive while the latter two are negative.

Good correlations between saturation magnetisation and coercivity on the one hand, and coercivity and susceptibility on the other hand, were achieved only after omitting the Trevorite sample, which possesses an anomalously high coercivity (>200 Oe) and sample KO-02 which has an anomalously low coercivity for its (low) saturation magnetisation and susceptibility. These latter quantities are negatively correlated with coercivity. The correlation coefficient for saturation magnetisation versus susceptibility is 0.866, for saturation magnetisation versus density it is 0.747, for saturation magnetisation versus coercivity it is 0.644 and for coercivity versus susceptibility it is 0.742.

3. Susceptibility versus Temperature

Comments on individual k-T curves, which are given in the appendix, are included in Table 1. Most samples are consistent with standard multi-domain (MD) magnetite, showing a peak near -150°C indicating the isotropic point, a fairly gentle increase with increasing temperature and a generally sharp drop just before 580°C, corresponding to the Curie point of magnetite. Several departures from this are apparent. Curves for S12, S15 and S16 show relatively steep increases of susceptibility with temperature reflecting the presence of significant ultra-fine superparamagnetic (SPM) magnetite. These grains are blocked (contributing dominantly to remanence) at lower temperatures and become progressively unblocked (contributing only to susceptibility) across a broad temperature spectrum. Some curves display a distictive hump around 300°C to 400°C (i.e. COMP17), which corresponds to a cation deficient phase (maghemite) possibly due to oxidisation. The Trevorite sample (QN01) is highly doped with nickel, which is reflected in its low Curie point. Another sample which displays a low Curie point is the sample of fly-ash (POZ01) which may be heavily doped with aluminium. It is well established that doping magnetite with cations of Ti, Ni and Al usually reduces Curie points.

4. HMS Properties

The three HMS magnetites, Biggenden, Savage River and Tasu, have a mean coercivity of 46 Oe, a mean (specific) saturation magnetisation of 86 emu/g, and a mean (mass) susceptibility of 0.025 emu/g. These values compare with ~30 Oe, 92 emu/g and 0.04 emu/g for pure MD magnetite respectively. Observed susceptibilities are subject to self-demagnetisation which accounts for the somewhat low values measured herein. The HMS samples have a mean density of 4.43 gcm^{-3} compared with pure magnetite of 5.18 gcm^{-3}. The relationship of saturation magnetisation versus susceptibility appears to be the best discriminator between pure magnetite and other compositions.

Table 1 Petrophysics of Magnetite Concentates

Sample	Mass	Density	Hc	Jrs/Js	Js(emu/g)	Sus (emu/	Curie T.	Comments
BB01	1.0025	4.066	10.43262	0.0097	79.39235	28990.32	580	Std MD mt curve; very soft
CMP10	1.0004	4.123	37.51528	0.0358	60.64202	20094	580	Std MD mt curve
CMP14	1.0012	4.025	87.57078	0.0782	53.47516	15502.08	570	MD Mt + SD mhm, high coercivity
CMP15	1	4.334	50.47702	0.0395	52.23718	16665.48	580	MD + SD mt
CMP16	0.9994	4.729	23.28898	0.016	69.27646	20743.05	580	MD mt (+ minor SD mt)
CMP17	0.9993	3.694	84.09324	0.109	37.27691	14061.72	570	MD mt + SD/SPM (?titano)mhm
COMP3	0.9997	4.856	23.49974	0.0158	75.66371	21678.86	570	Std MD mt curve + ?
COMP6	1.0018	4.353	45.62954	0.0397	61.74103	18473.63	570	Std MD mt curve + ?
COMP9	0.9996	3.653	69.5508	0.0987	37.46345	15080.67	570	V.sim 17
HO1C1	1.0019	4.702	92.62902	0.0936	37.94606	12574.31	575	PSD mt
KO-02	1.0016	2.506	40.88744	0.0413	10.80452	4301.238	580	Std MD curve
NTPR1	1.0066	4.217	71.76378	0.0811	42.13482	15203.26	560-600	Rg of comps
POZ1	1	3.688	116.757	0.126	41.63706	12808.8	450-550	(?) Aluminous SD +SPM
QMO2	1.0054	3.243	49.5286	0.0602	49.3663	17000.28	550	MD mt curve with high isotropic pt
QN01	0.997	3.795	203.1726	0.295	36.01019	12347.96	500-530	Nickeliferous; very hard
S12C1	0.9954	3.069	96.52808	0.219	22.41406	11886.08	560-580	V.fine mt (SPM + SD)
S12C3	0.5005	3.069	96.21194	0.218	23.34561	12036.44		
S15C1	1.0007	3.224	98.84644	0.184	24.73518	12136.1	560-580	V.sim 12
S15C3	0.501	3.224	99.16258	0.205	27.24417	13647.66		
S16C1	1.0022	3.143	109.7006	0.212	22.02997	10143.72	560-580	V.sim 12
S19C1	1	4.647	29.08488	0.0234	68.81635	20156.04	580	Std MD mt curve
S20C1	0.998	4.484	21.076	0.0151	74.13835	21763.41	570	Std MD mt curve
S22C1	1.0026	4.865	26.02886	0.0209	73.99533	23135.01	580	Std MD mt curve
S25	1.0011	4.398	61.777	0.055	61.32051	18792.93	580	Std MD + PSD mt curve, higher coercivity
S26C1	1.0013	4.49	59.85584	0.048	56.89514	17644.78	580	Std MD mt curve
WW1-1	1.9951	4.72	38.67446	0.053	74.11352	17645	570	Std MD mt curve with hg iso pt
WW1-2	1.9951	4.72	38.4637	0.0398	71.88743	22843.97		
WW1-3	1.0008	4.72	40.06	0.035124	72.48743	22786.2		
SRiver	1.0001	4.642	62.5	0.0486	89.72422	23948.77		
TASU	1.0003	4.636	63.85	0.048	87.81717	22435.67		

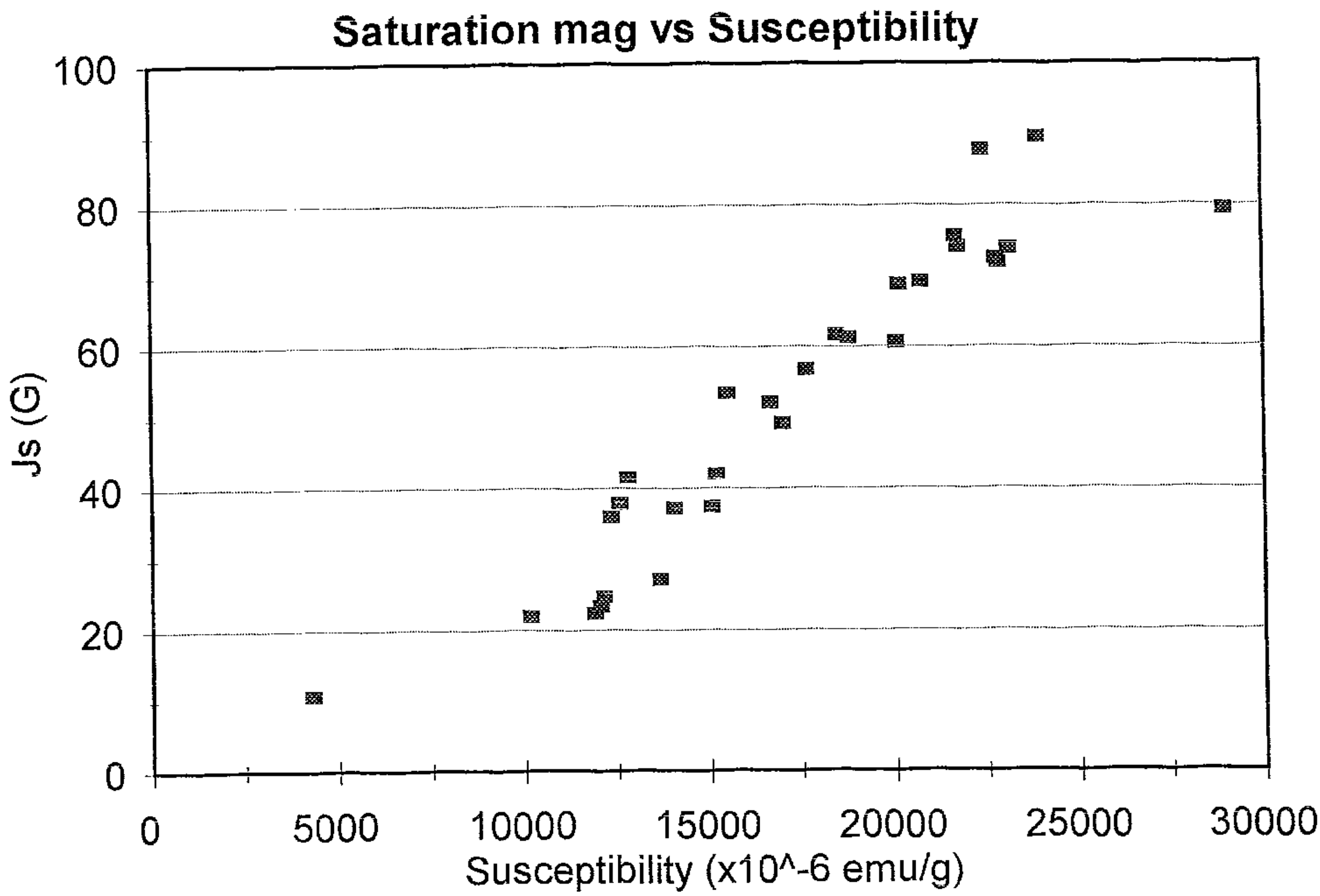

Figure 1. Plot of saturation magnetisation (Gauss) versus susceptibility ($\times 10^{-6}$ emu/g)

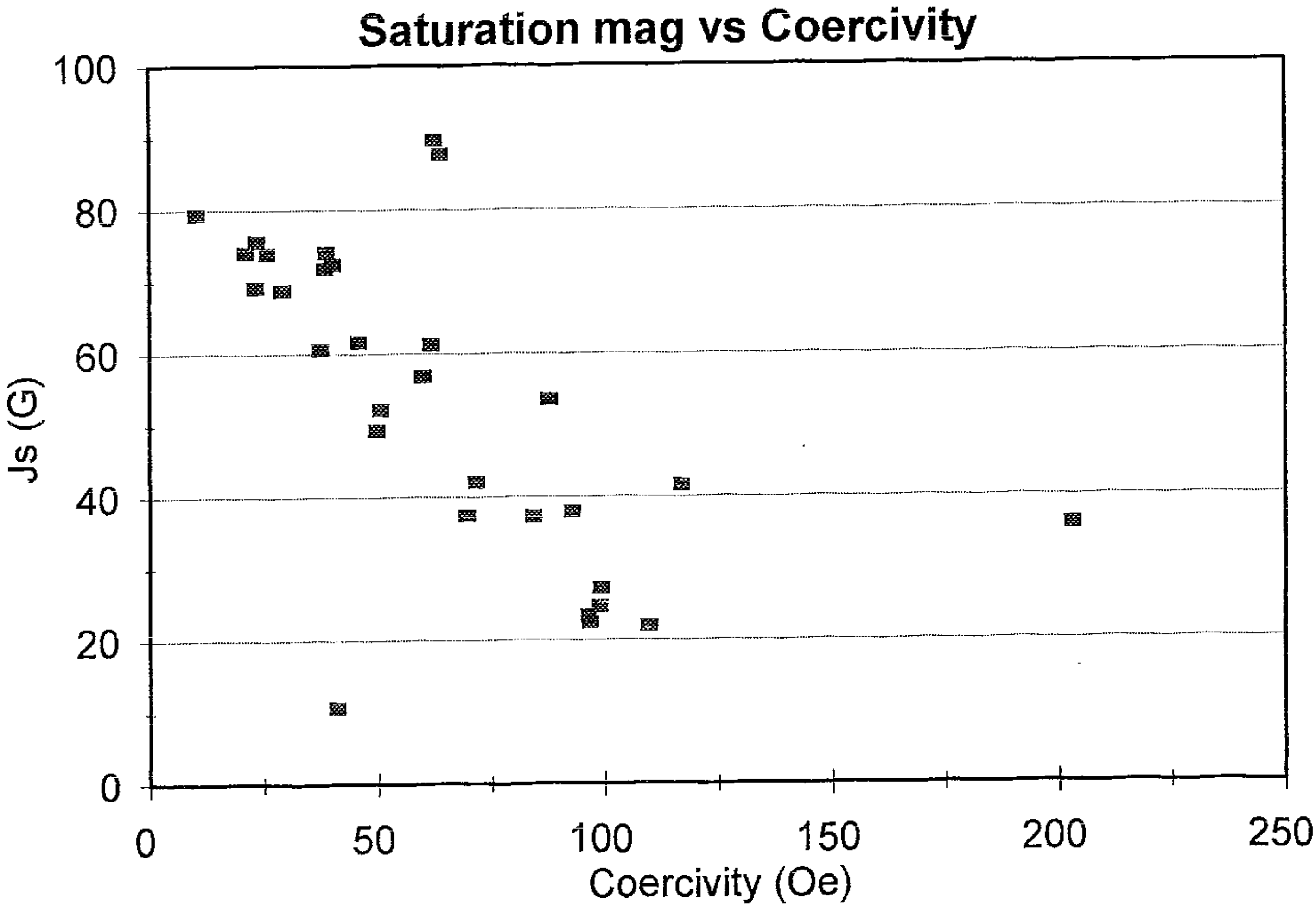

Figure 2. Plot of saturation magnetisation (Gauss) versus coercivity (Oersteds)

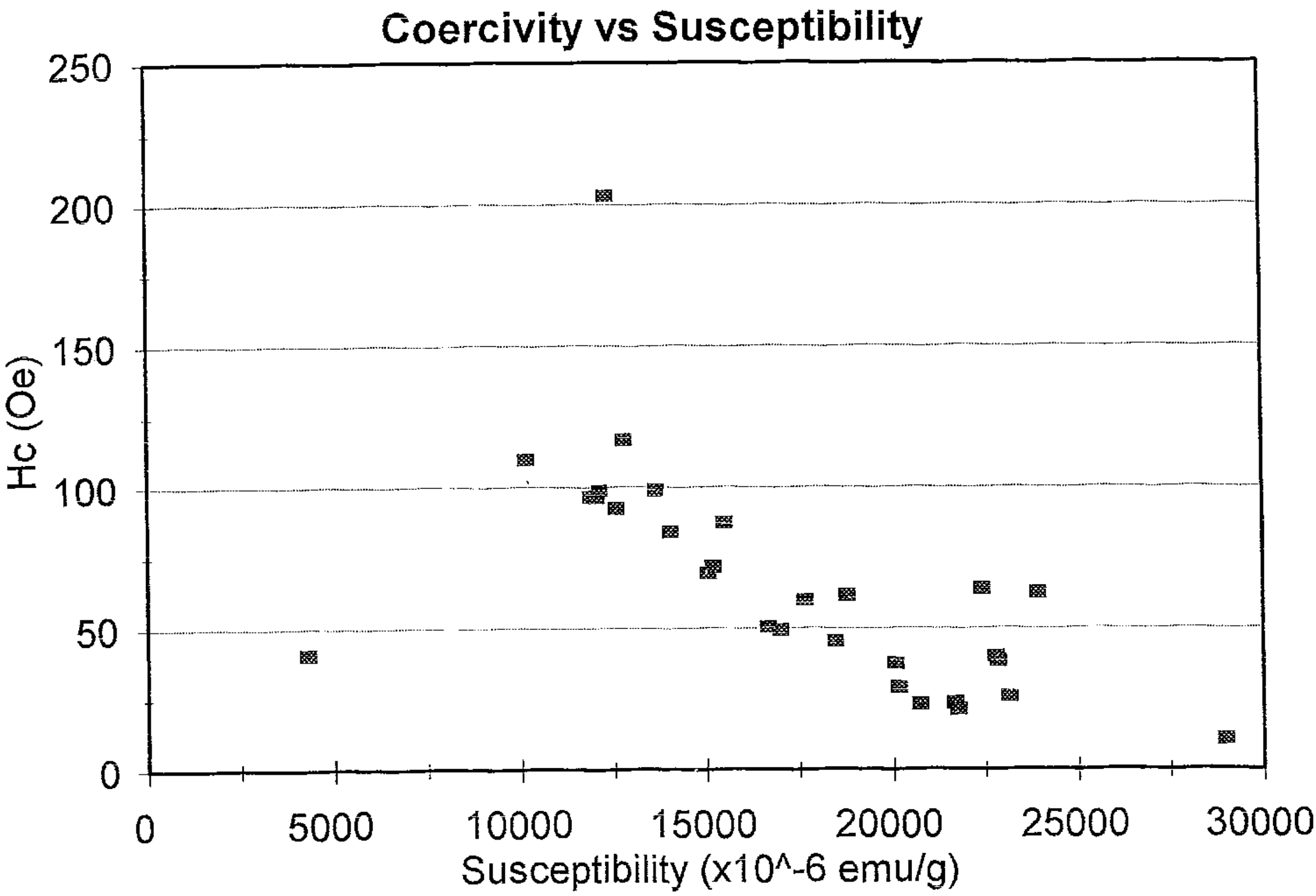

Figure 3. Plot of coercivity (Oersteds) versus susceptibility ($\times 10^{-6}$ emu/g)

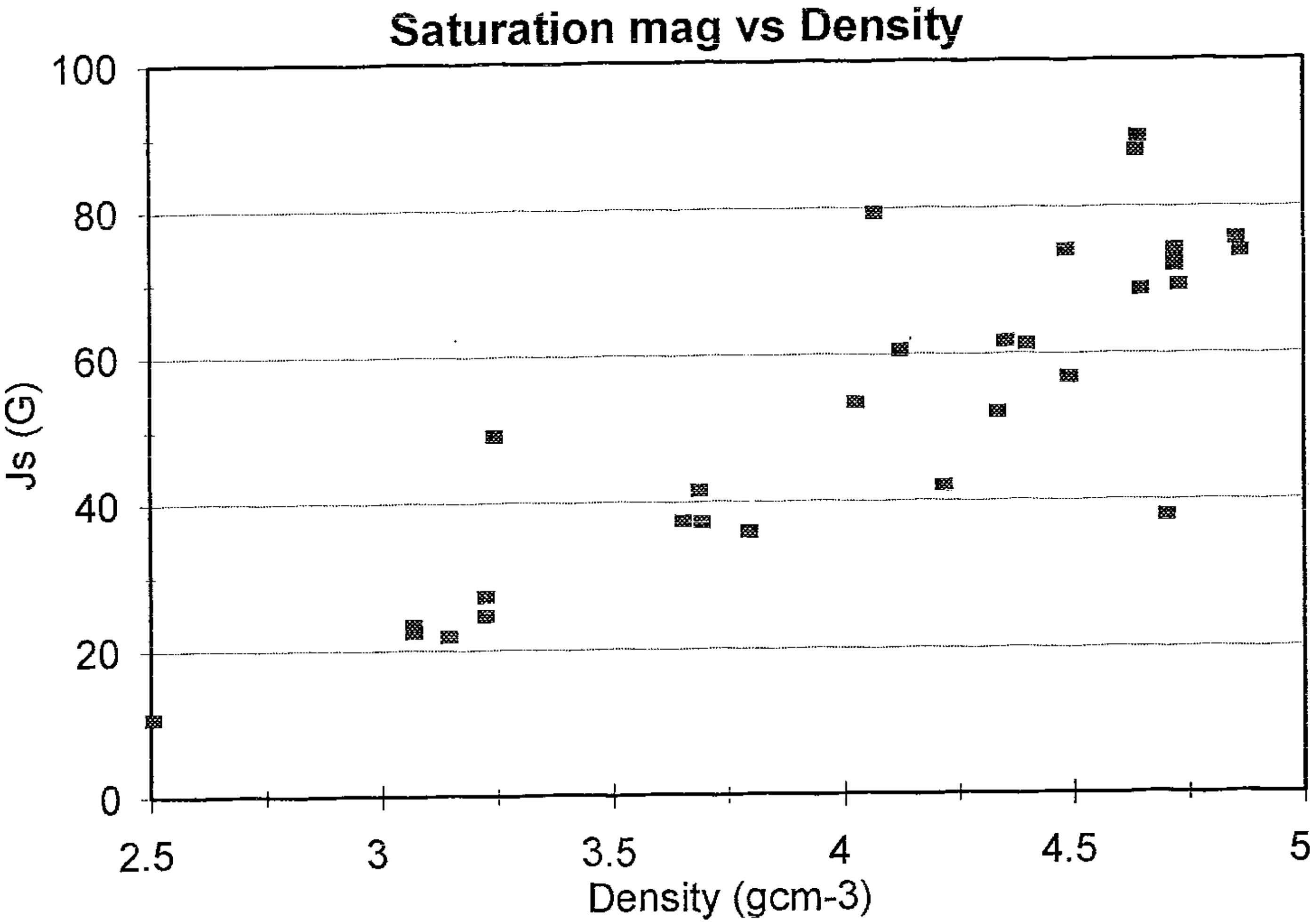

Figure 4. Plot of saturation magnetisation (Gauss) versus density (gcm^{-3})

Appendix - Hysteresis and Susceptibility/Temperature Plots

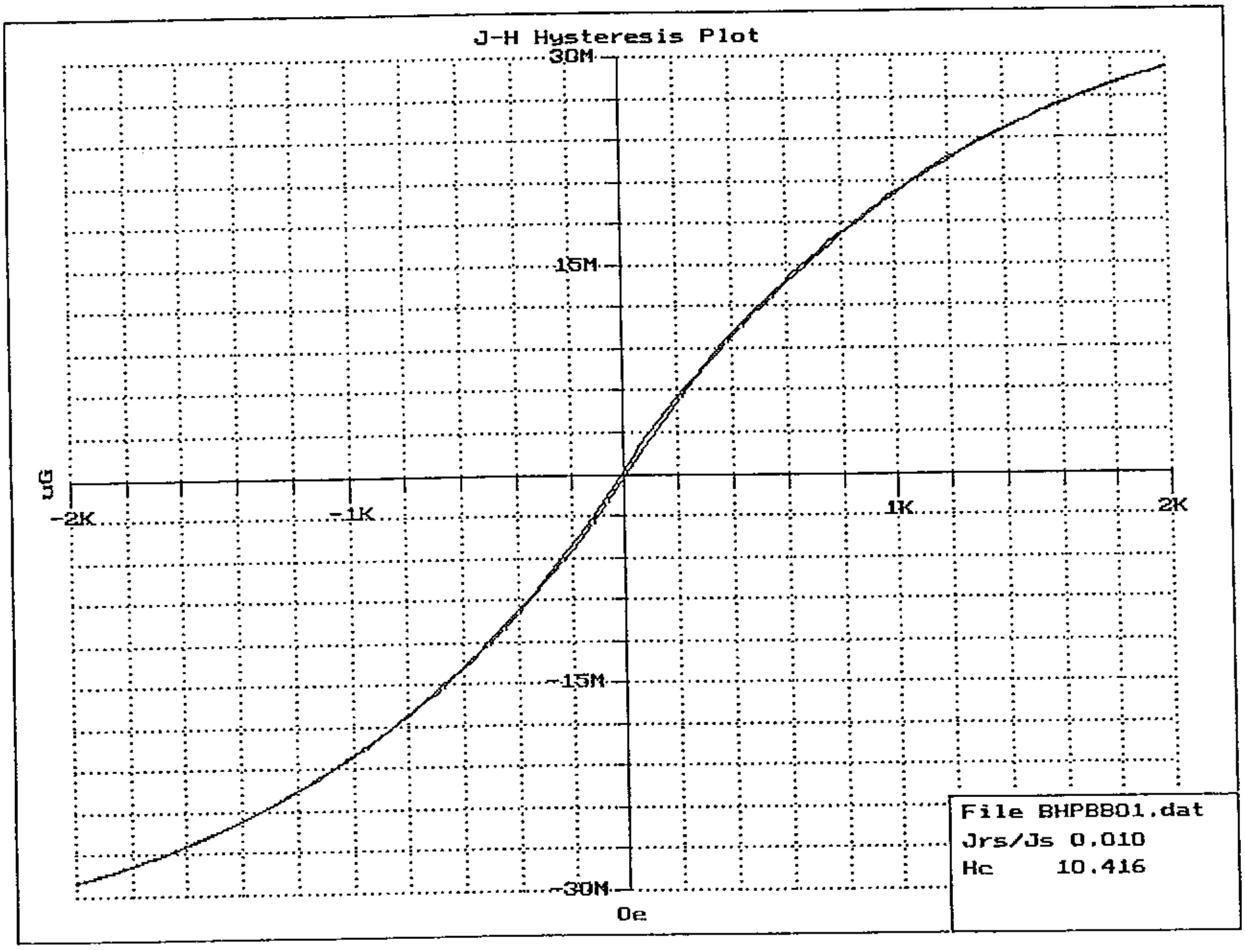

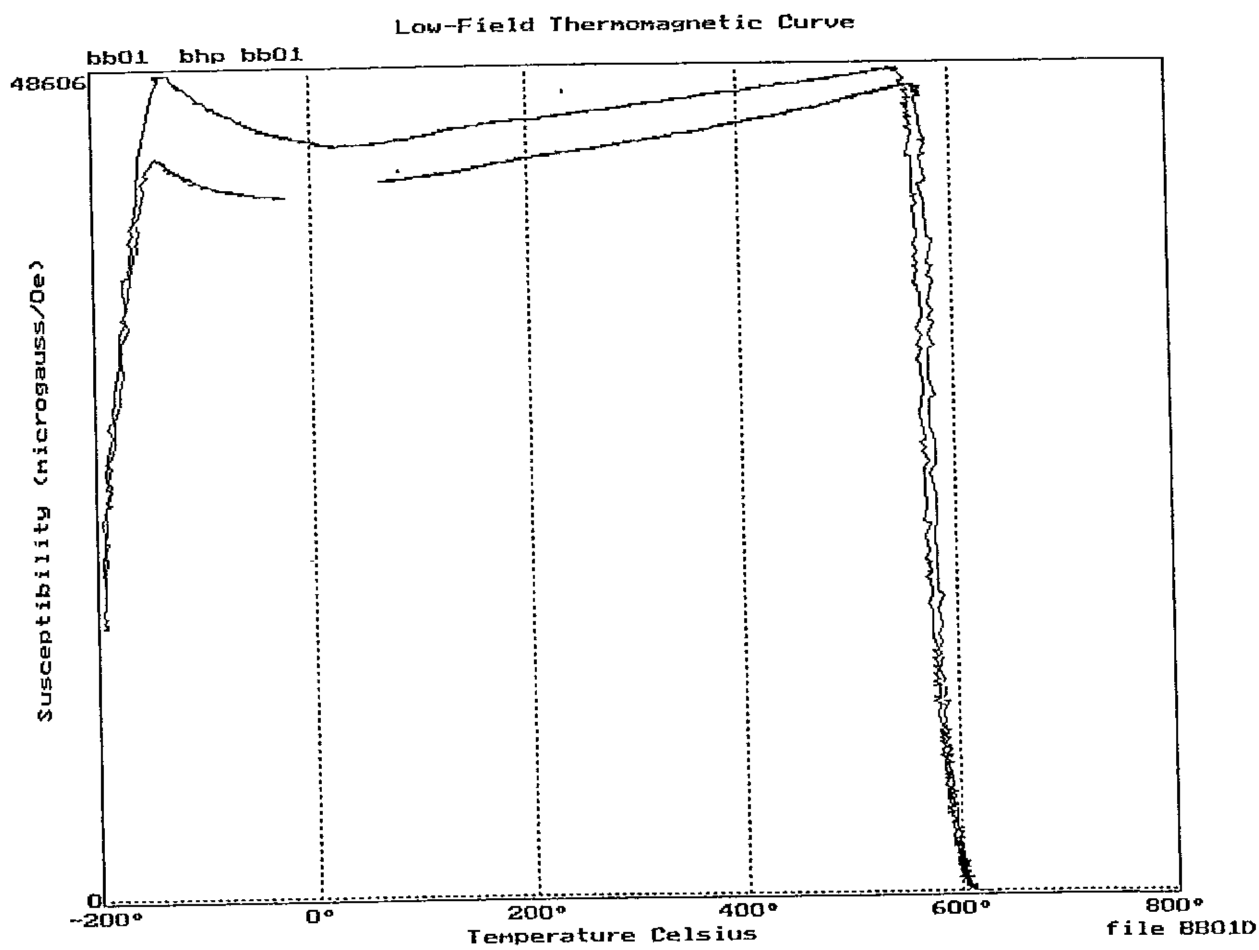

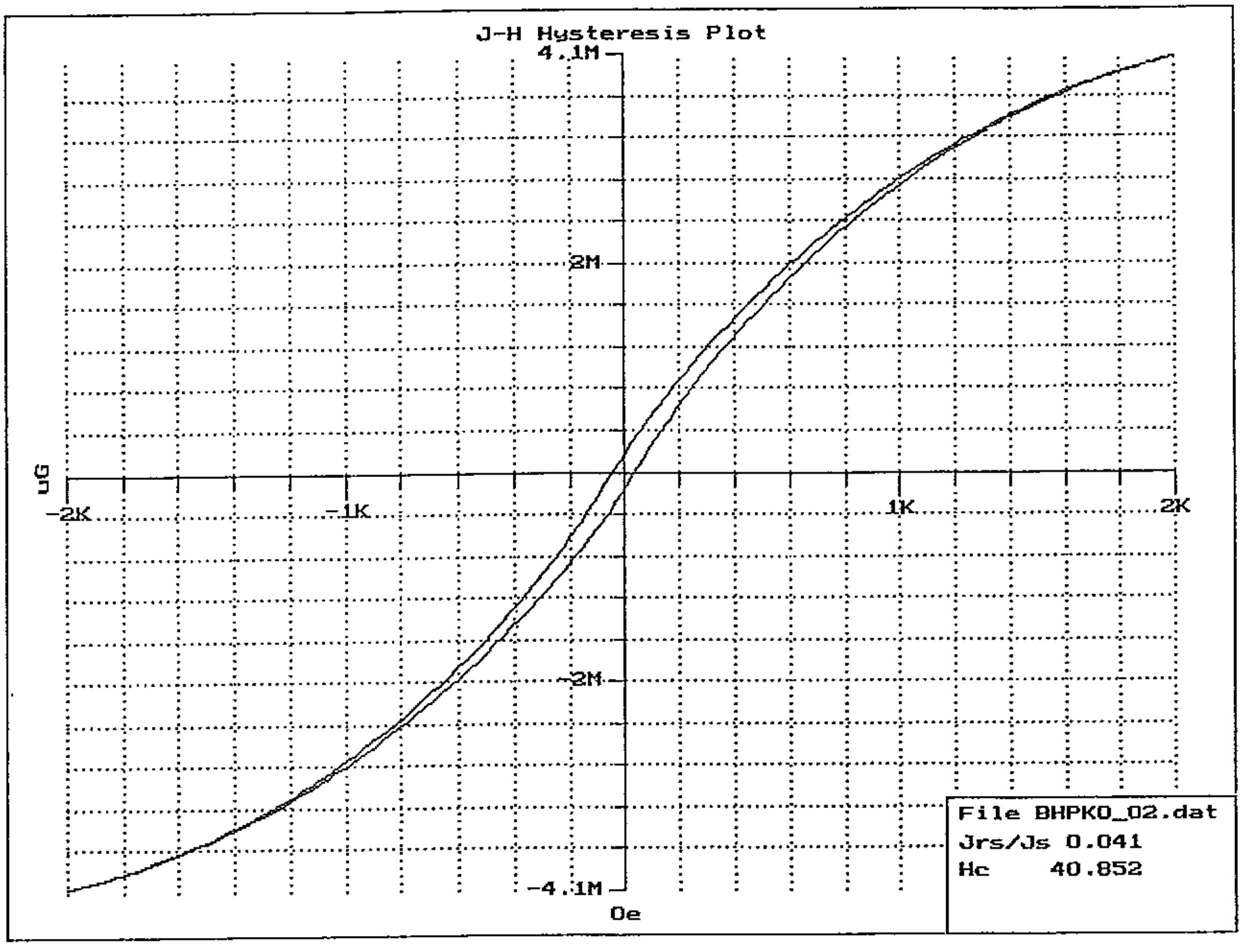
J-H Hysteresis Plot
4.1M
2M
-2M
-4.1M
uG
-2K
-1K
1K
2K
Oe
File BHPKO_02.dat
Jrs/Js 0.041
Hc 40.852

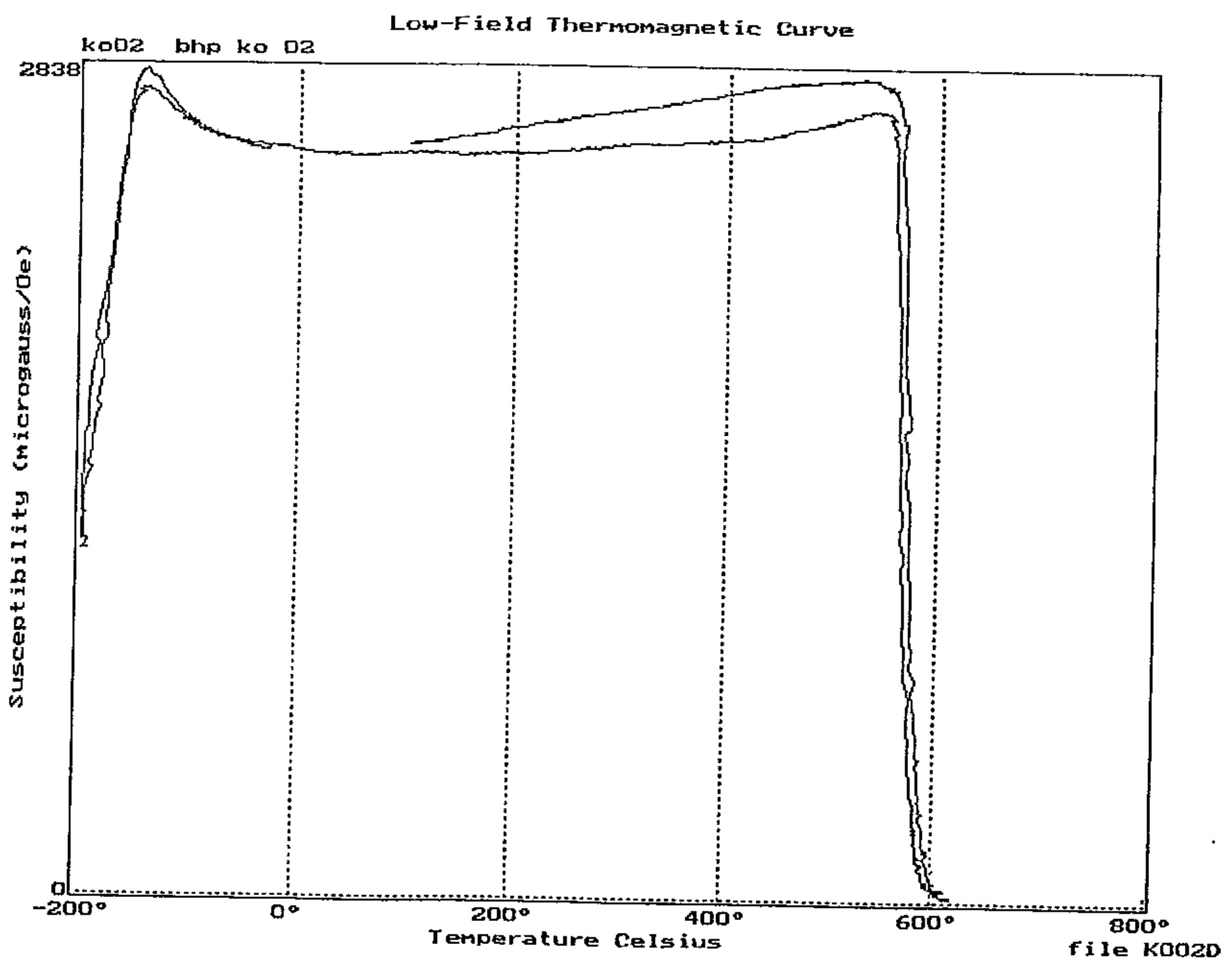
Low-Field Thermomagnetic Curve
ko02 bhp ko 02
2838
0
Susceptibility (microgauss/Oe)
-200°
0°
200°
400°
600°
800°
Temperature Celsius
file K002D

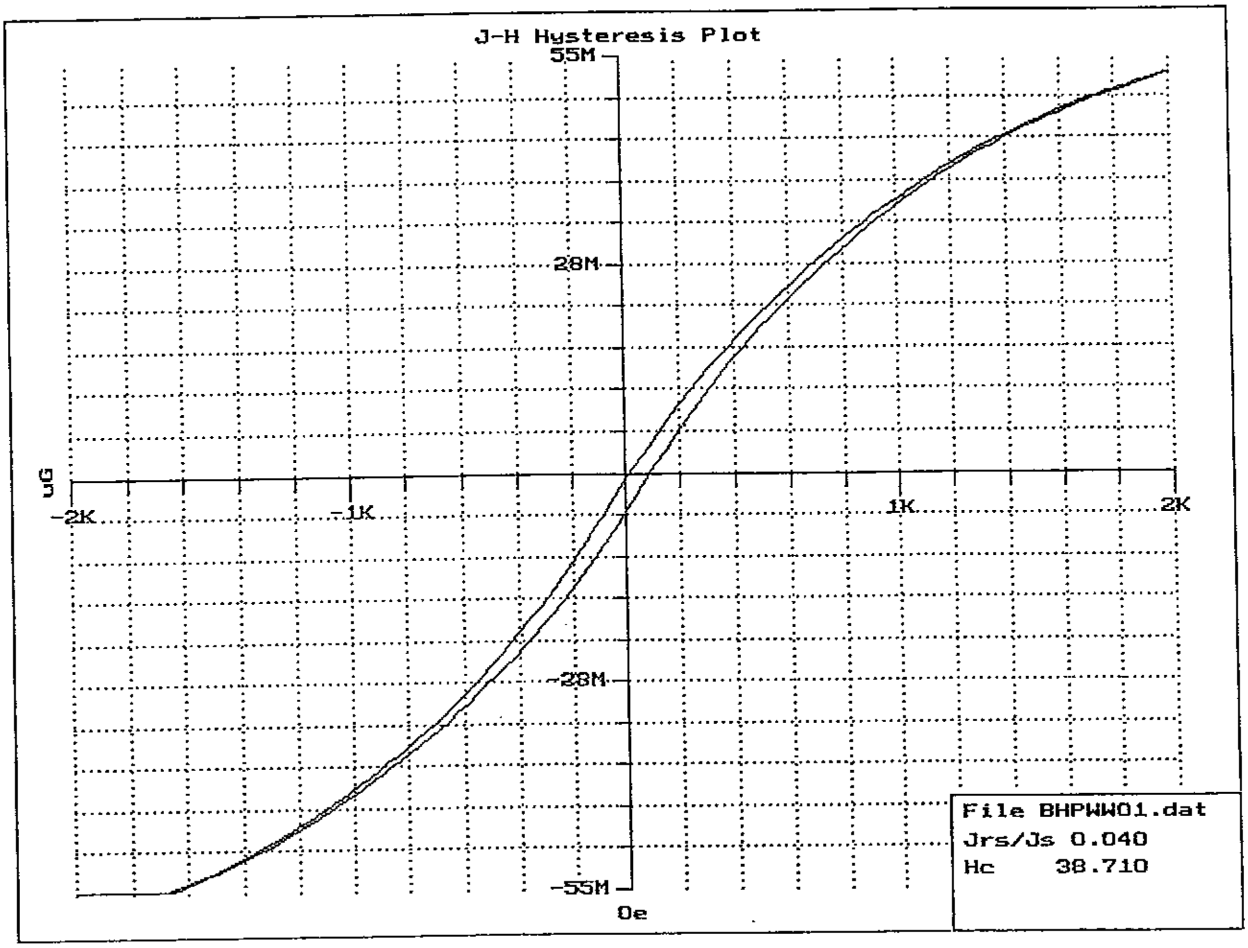
J-H Hysteresis Plot
55M
28M
uG
-2K
-1K
1K
2K
-28M
-55M
Oe
File BHPWW01.dat
Jrs/Js 0.040
Hc 38.710

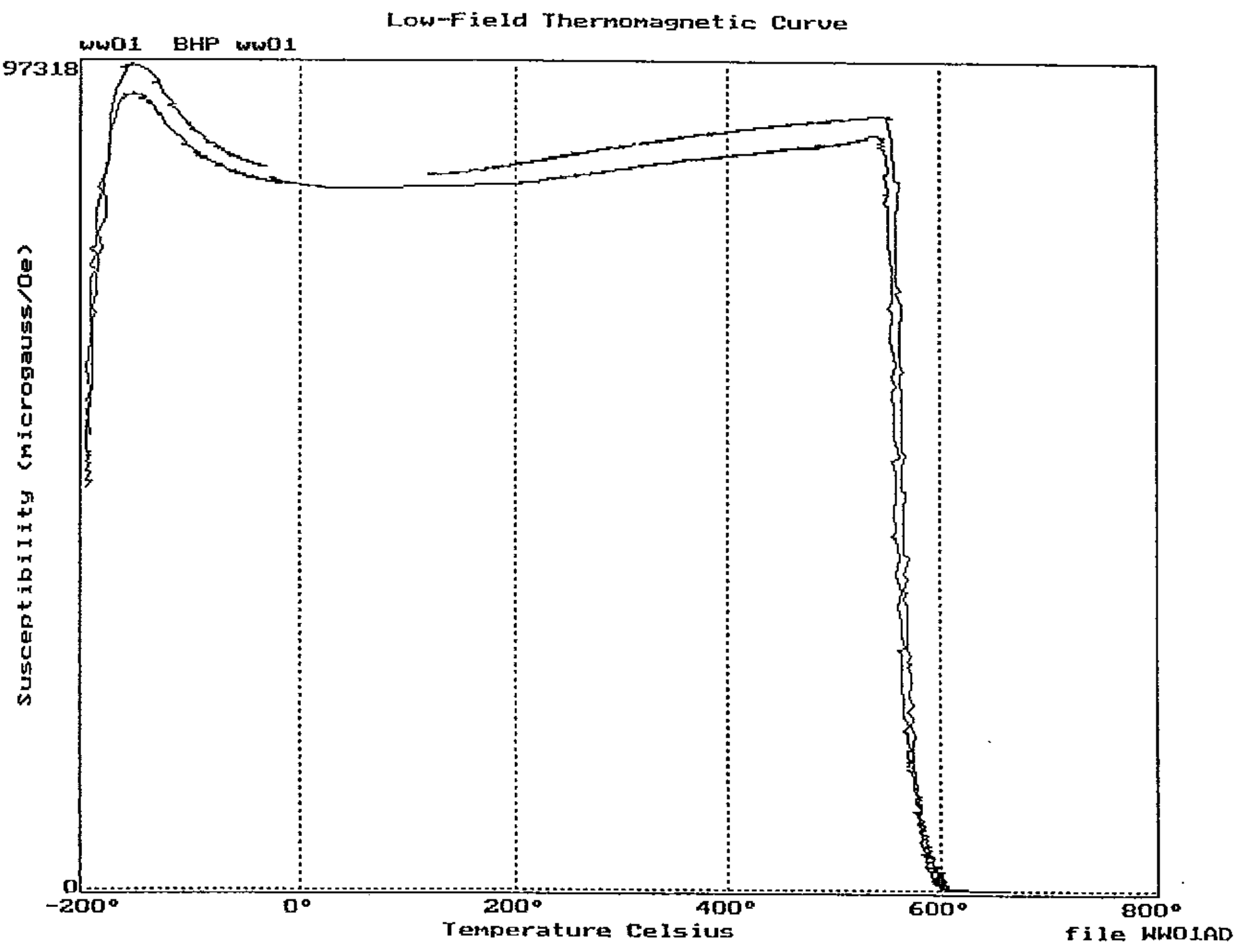
Low-Field Thermomagnetic Curve
ww01 BHP ww01
97318
Susceptibility (microgauss/Oe)
0
-200°
0°
200°
400°
600°
800°
Temperature Celsius
file WW01AD

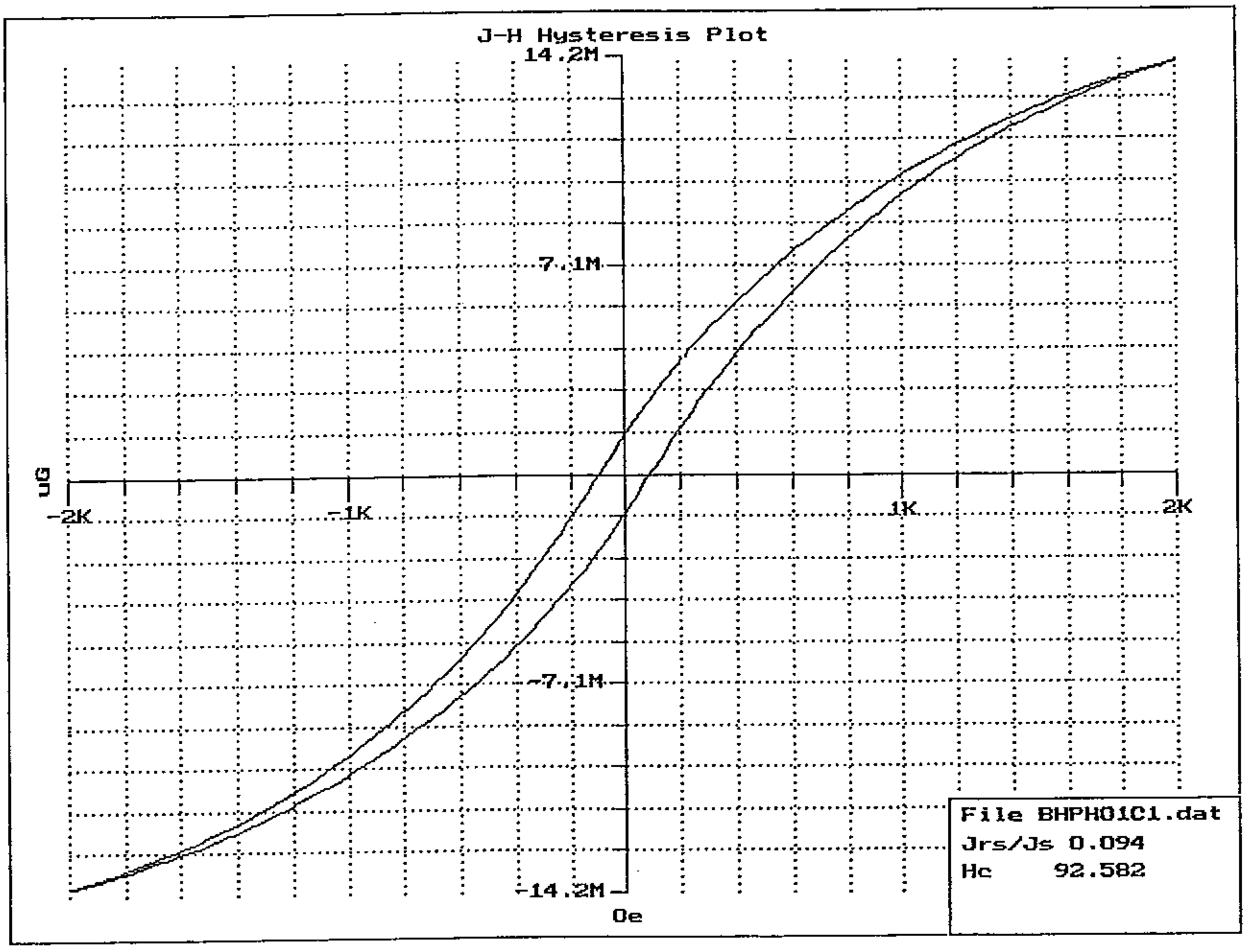
J-H Hysteresis Plot
14.2M
7.1M
-7.1M
-14.2M
uG
-2K
-1K
1K
2K
Oe
File BHPH01C1.dat
Jrs/Js 0.094
Hc 92.582

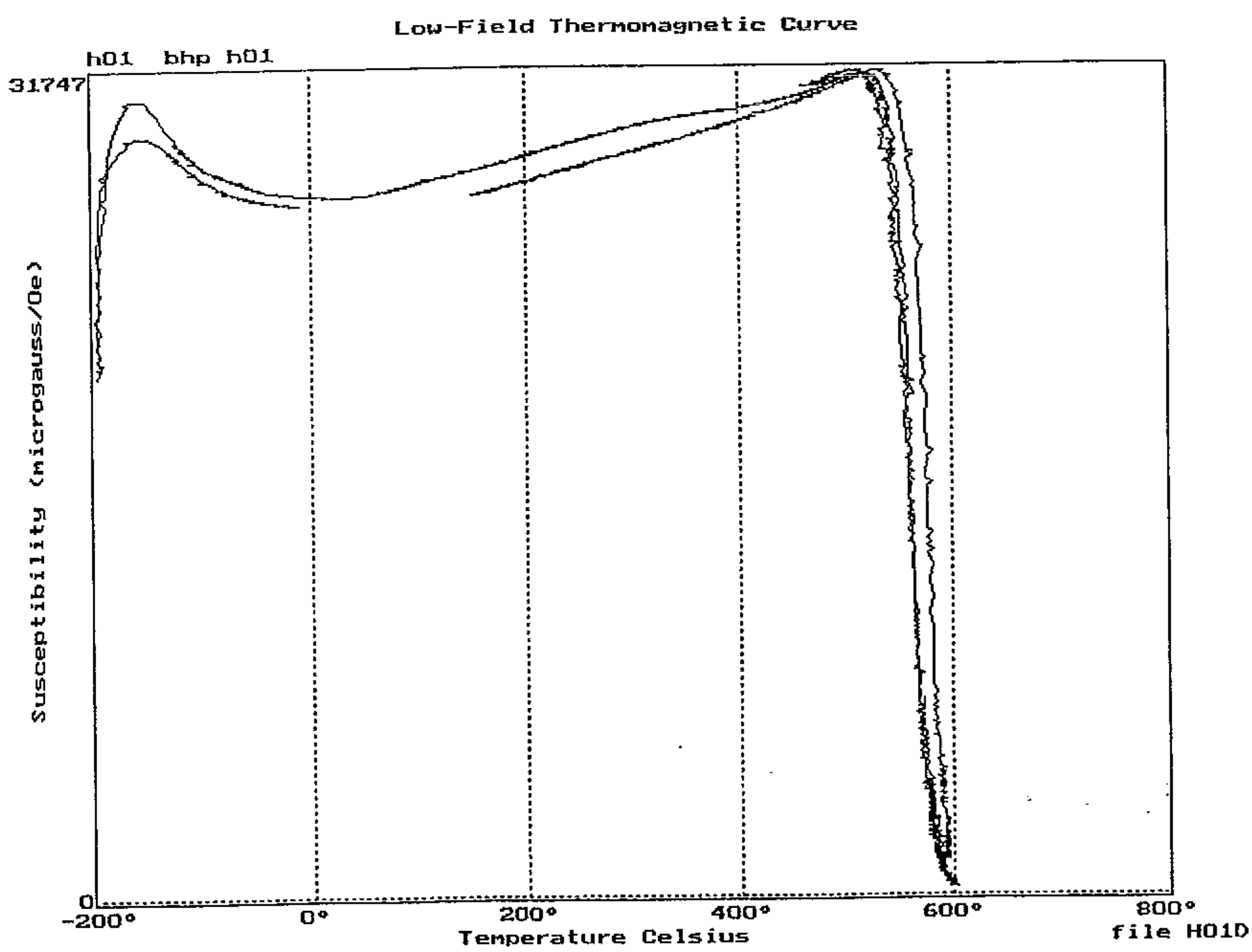
Low-Field Thermomagnetic Curve
h01 bhp h01
31747
0
Susceptibility (microgauss/Oe)
-200°
0°
200°
400°
600°
800°
Temperature Celsius
file H01D

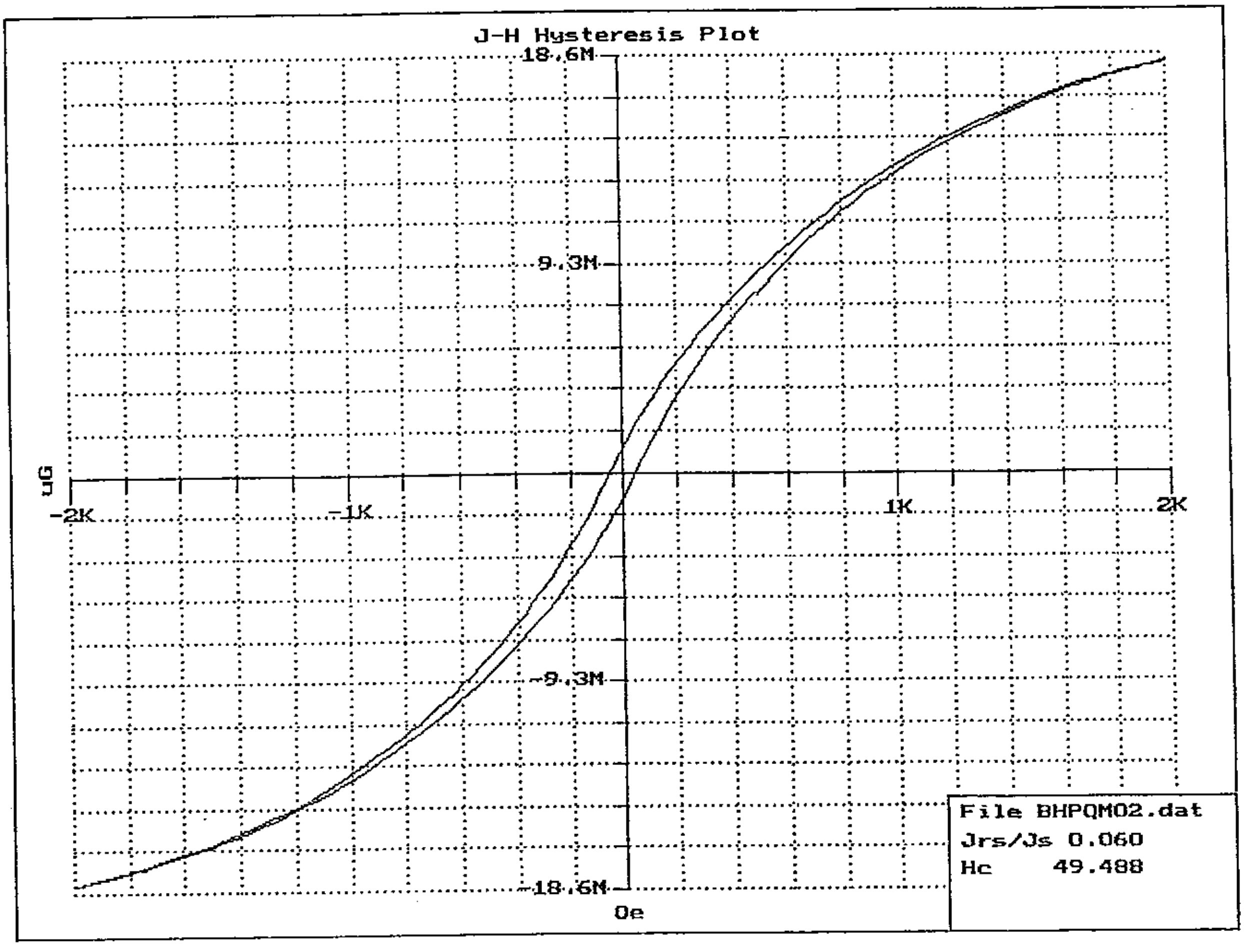
J-H Hysteresis Plot
18.6M
9.3M
-9.3M
-18.6M
uG
-2K
-1K
1K
2K
Oe
File BHPQM02.dat
Jrs/Js 0.060
Hc 49.488

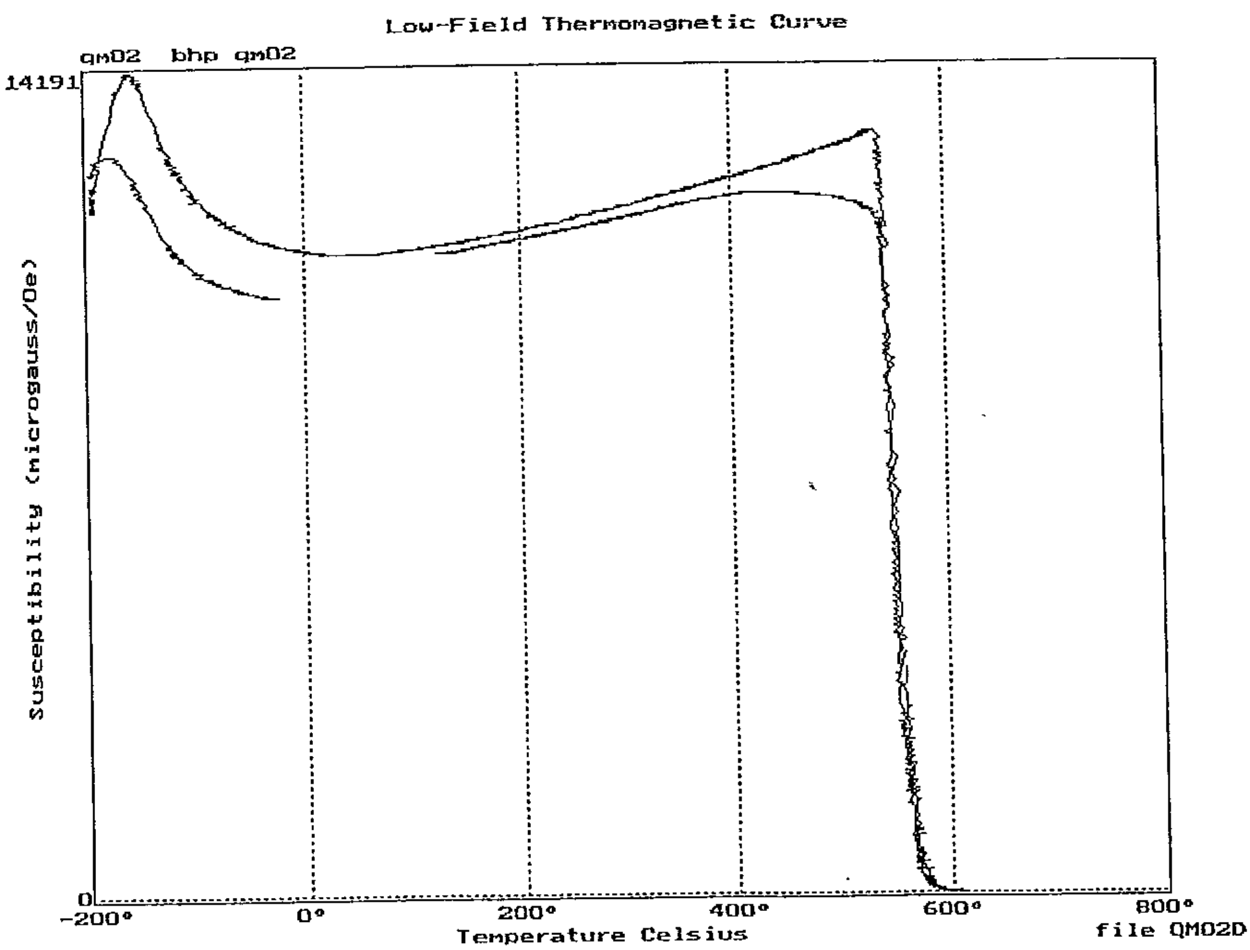
Low-Field Thermomagnetic Curve
qm02 bhp qm02
14191
0
Susceptibility (microgauss/Oe)
-200°
0°
200°
400°
600°
800°
Temperature Celsius
file QM02D

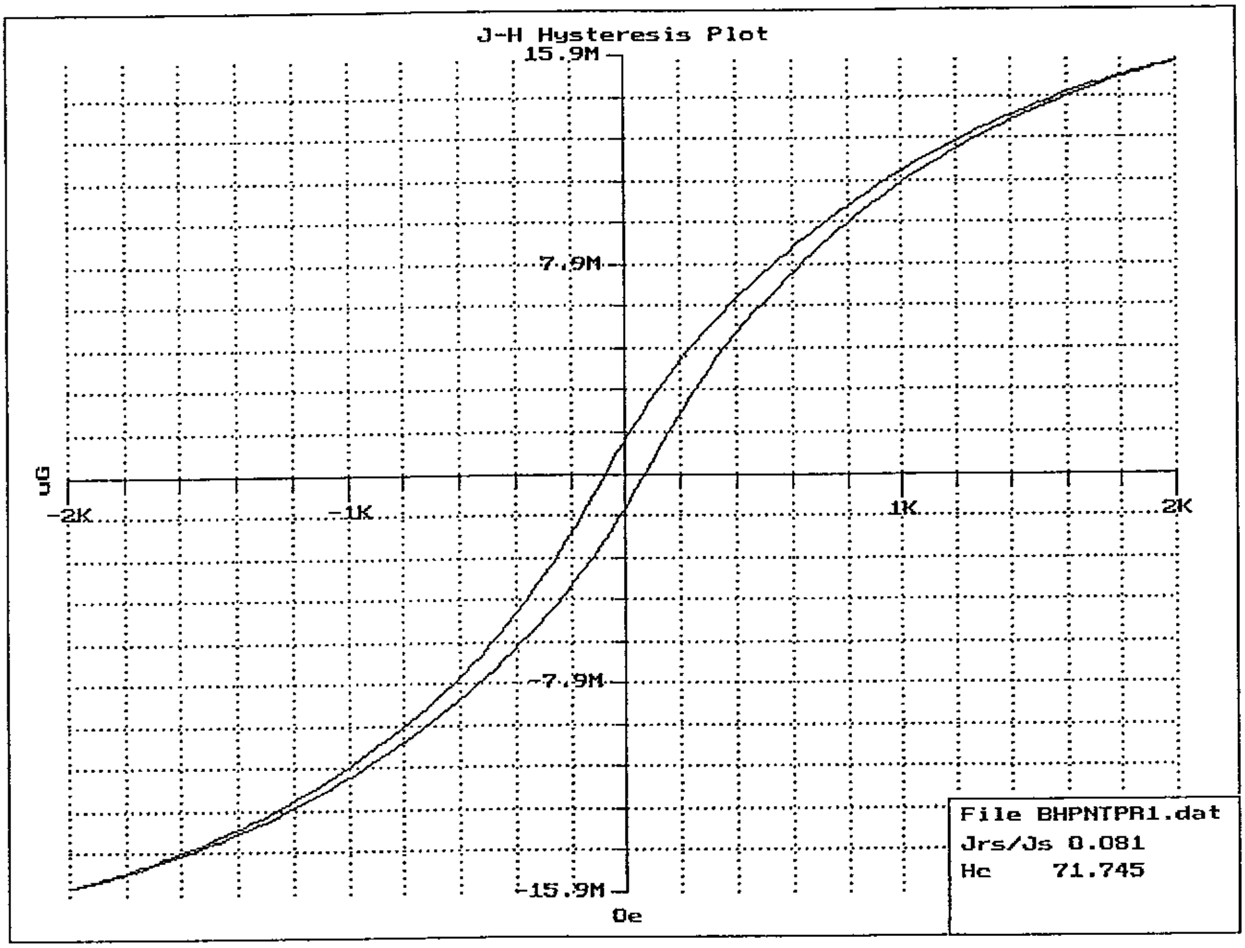
J-H Hysteresis Plot
15.9M
7.9M
-7.9M
-15.9M
uG
-2K
-1K
1K
2K
Oe
File BHPNTPR1.dat
Jrs/Js 0.081
Hc 71.745

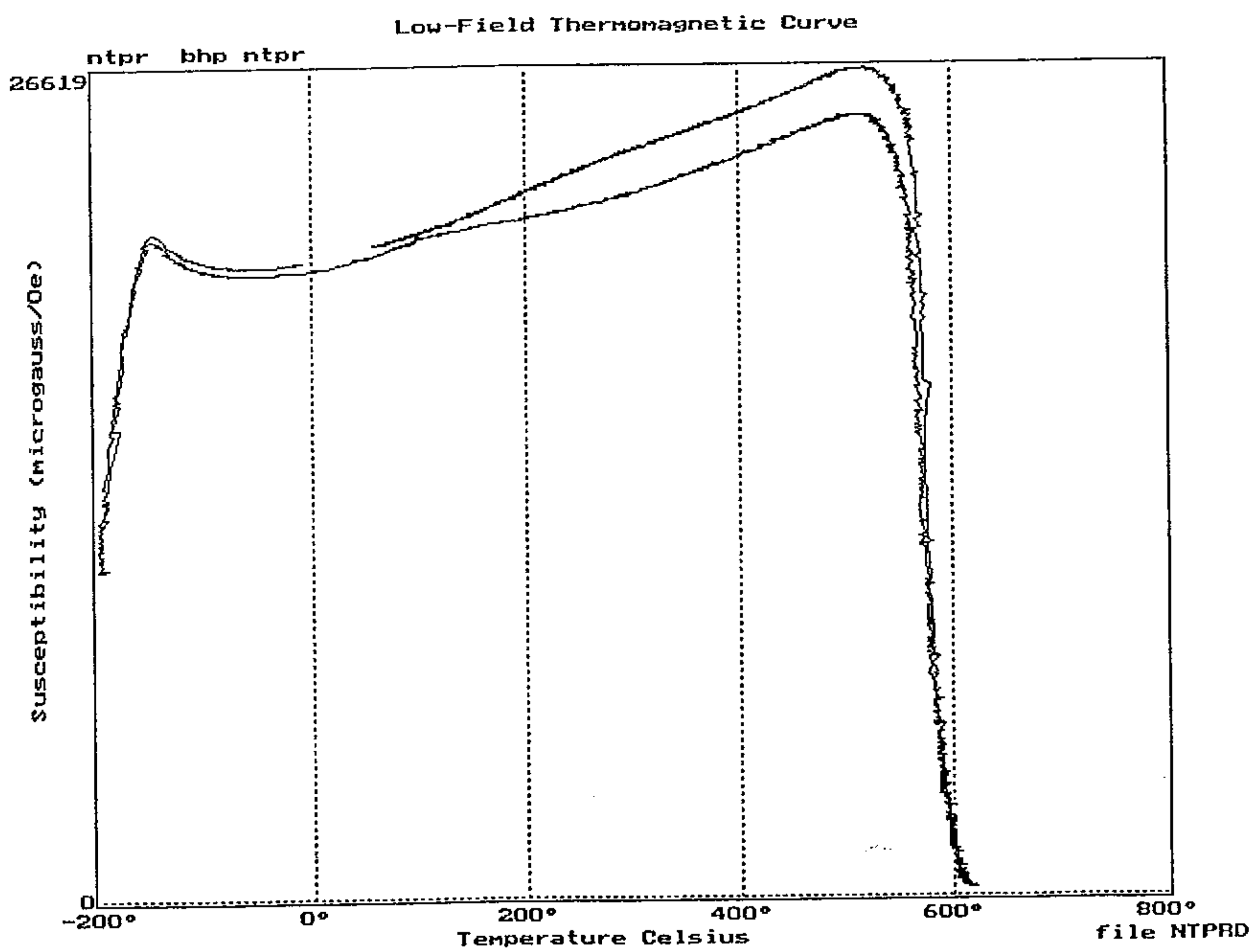
Low-Field Thermomagnetic Curve
ntpr bhp ntpr
26619
0
Susceptibility (microgauss/Oe)
-200°
0°
200°
400°
600°
800°
Temperature Celsius
file NTPRD

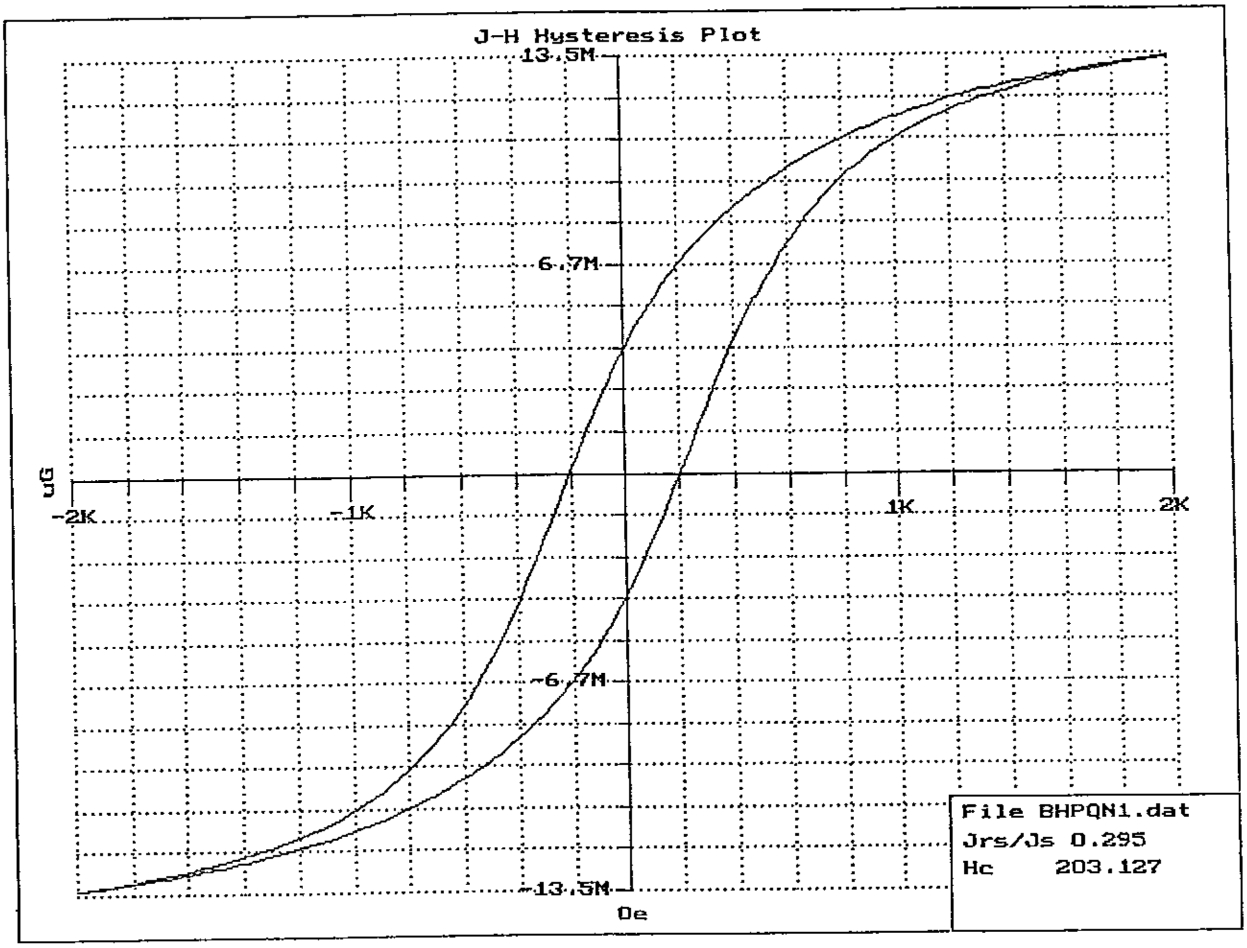
J-H Hysteresis Plot
13.5M
6.7M
-6.7M
-13.5M
uG
-2K
-1K
1K
2K
Oe
File BHPQN1.dat
Jrs/Js 0.295
Hc 203.127

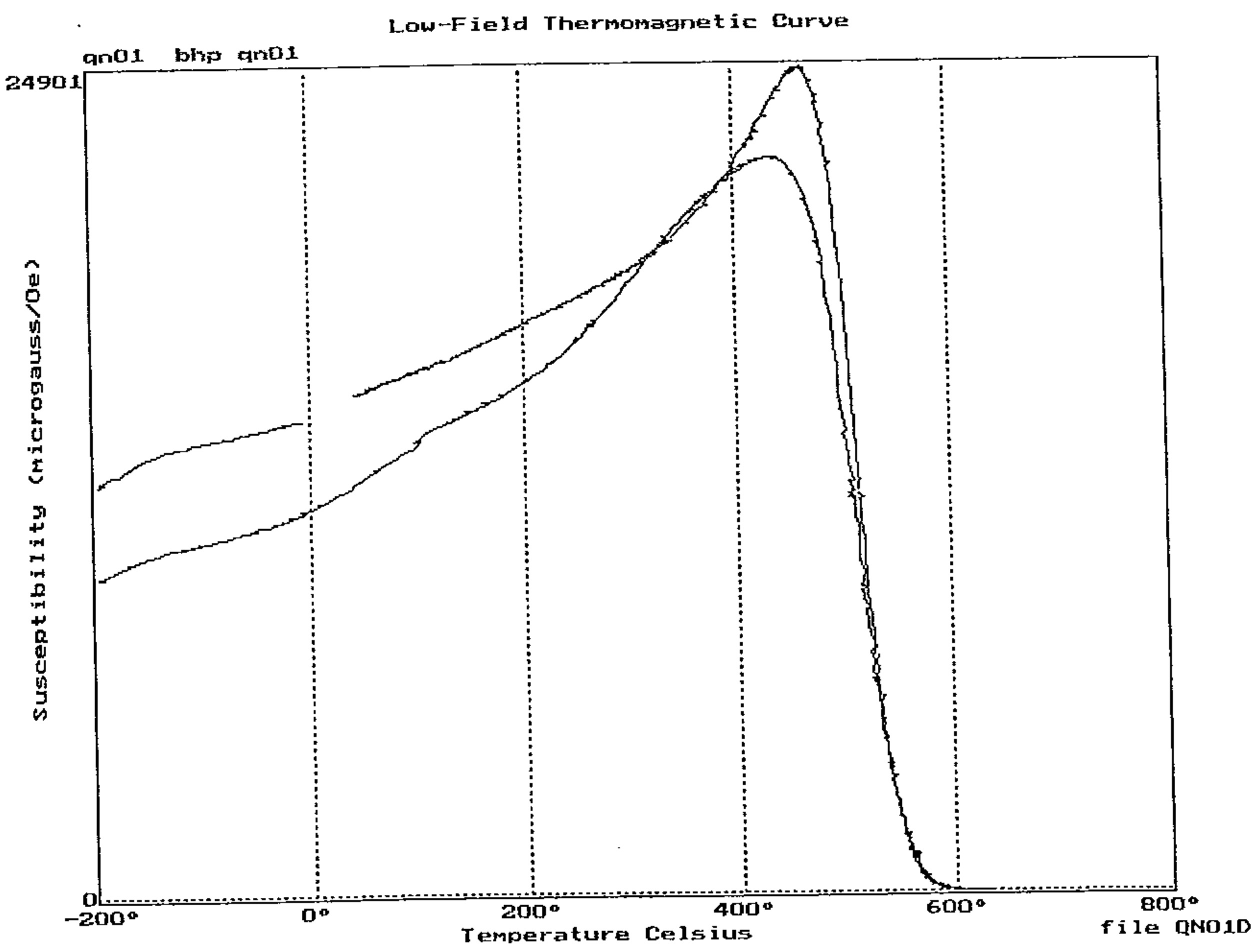
Low-Field Thermomagnetic Curve
qn01 bhp qn01
24901
0
Susceptibility (Microgauss/Oe)
-200°
0°
200°
400°
600°
800°
Temperature Celsius
file QN01D

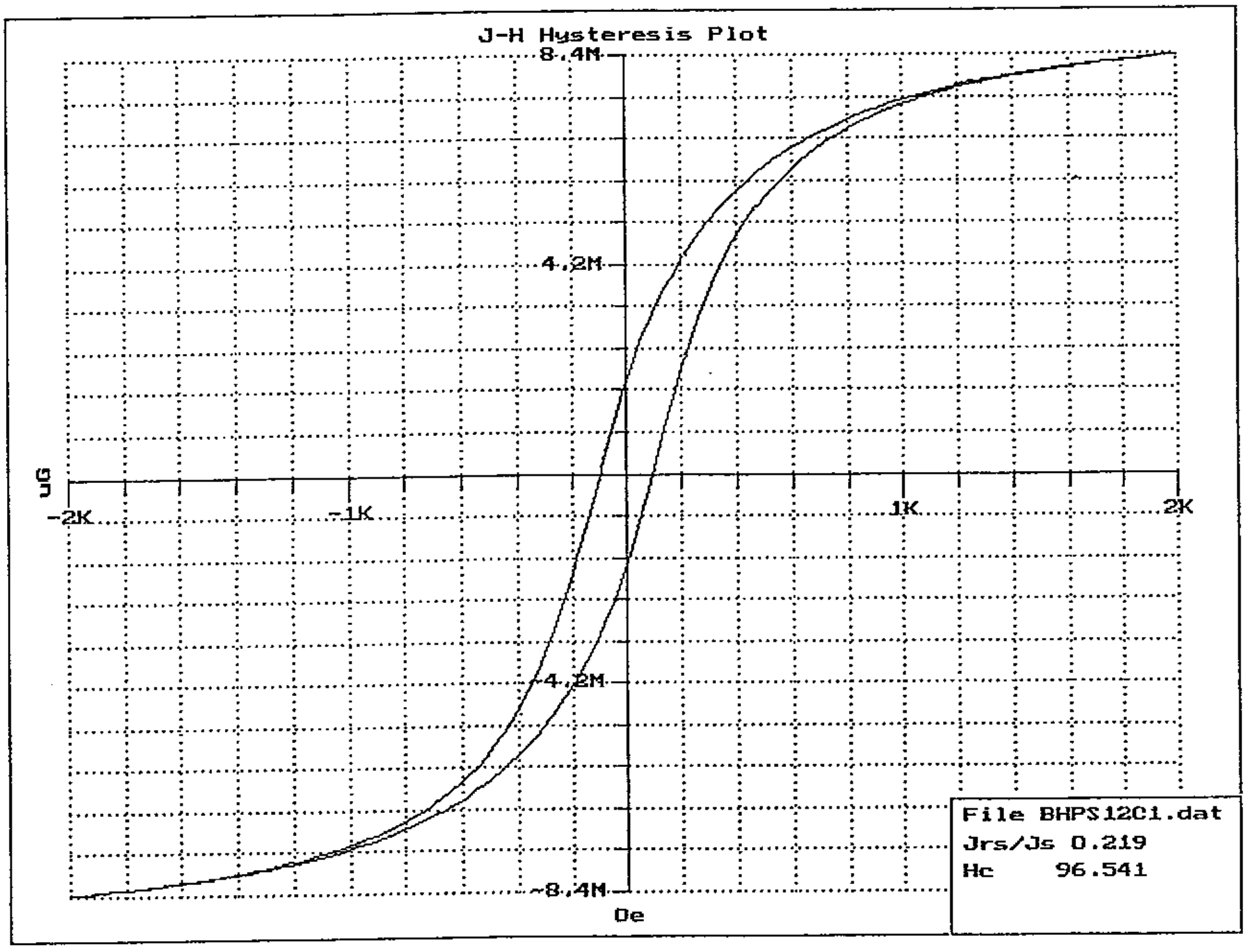
J-H Hysteresis Plot
8.4M
4.2M
-4.2M
-8.4M
uG
-2K
-1K
1K
2K
Oe
File BHPS12C1.dat
Jrs/Js 0.219
Hc 96.541

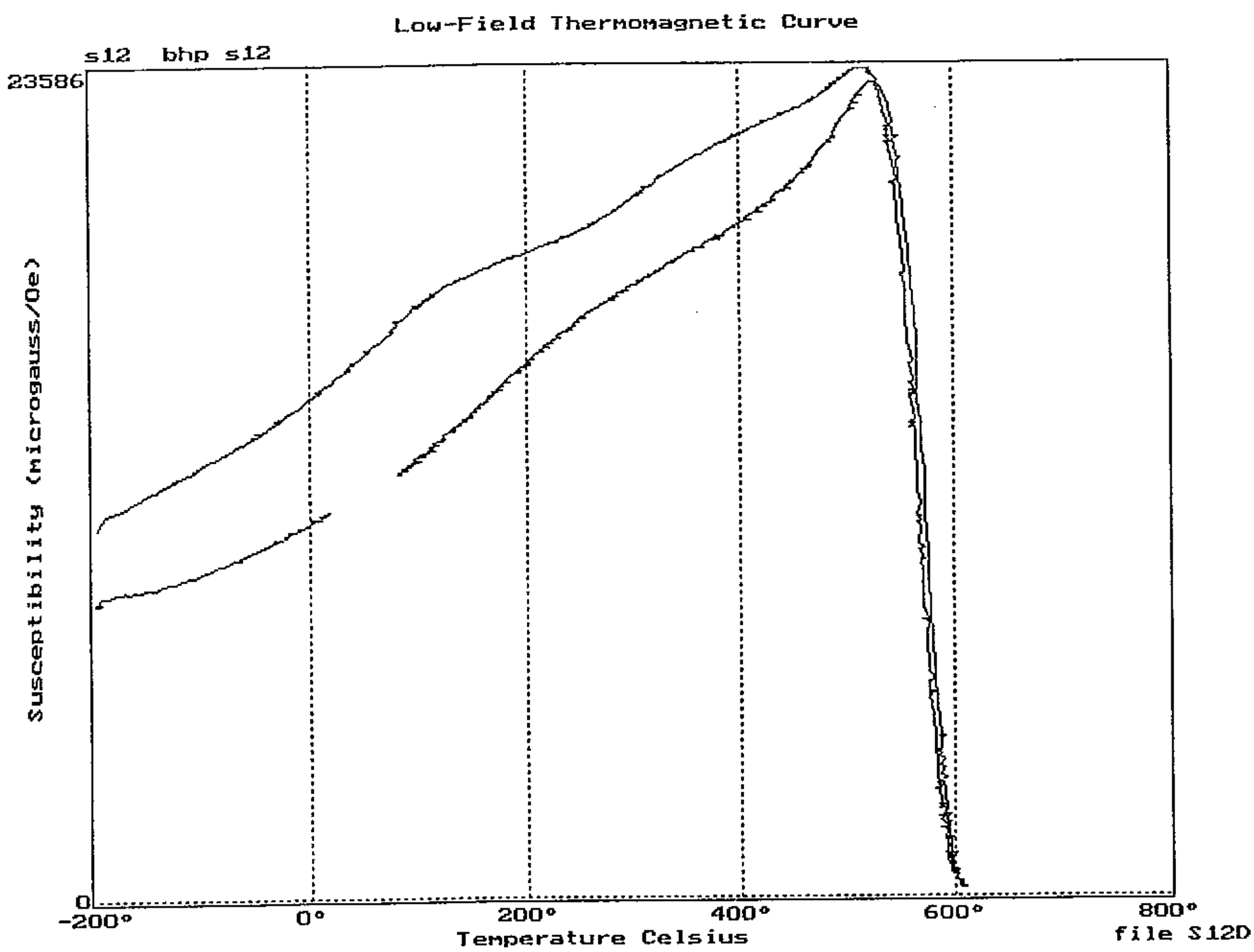
Low-Field Thermomagnetic Curve
s12 bhp s12
23586
0
Susceptibility (microgauss/Oe)
-200°
0°
200°
400°
600°
800°
Temperature Celsius
file S12D

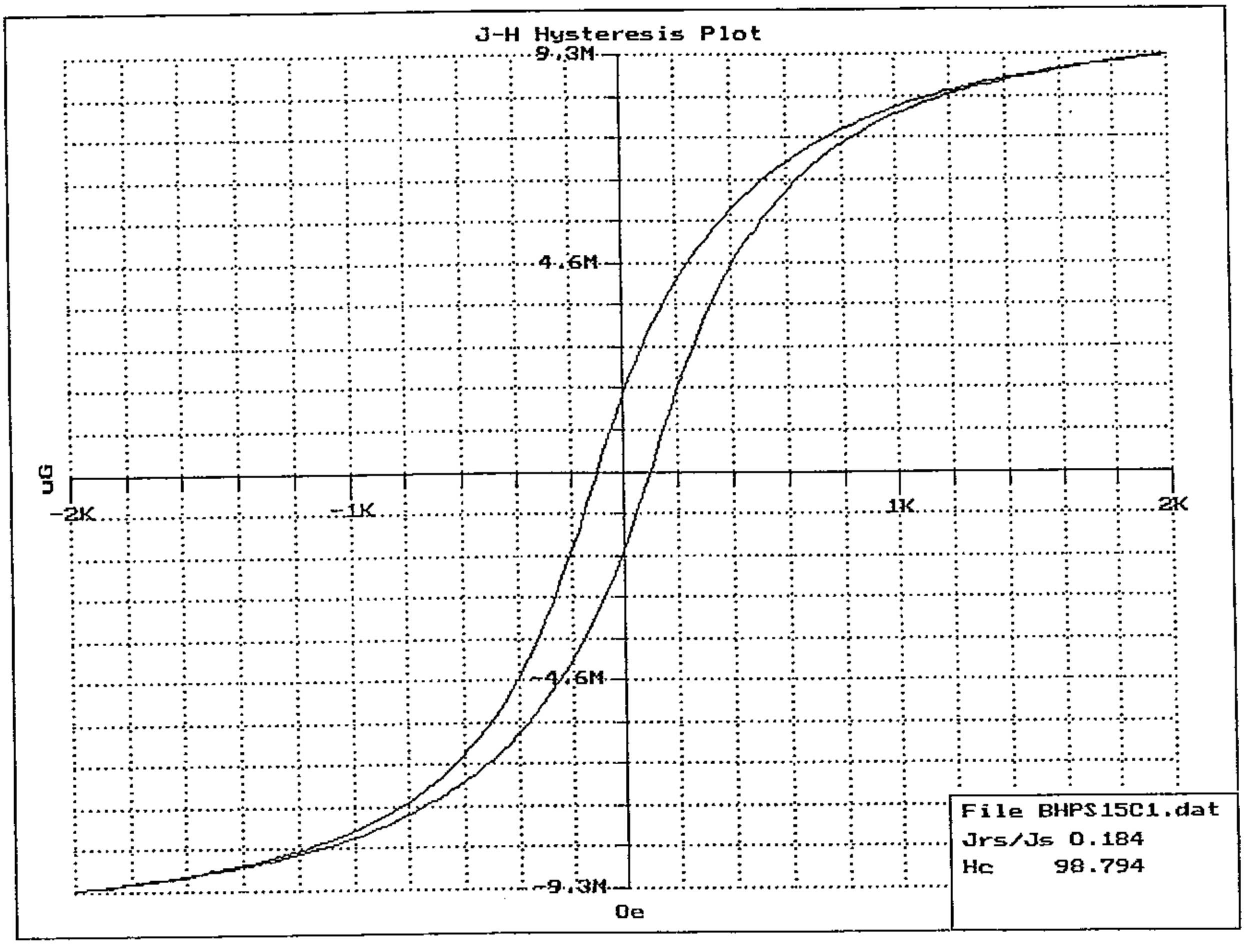
J-H Hysteresis Plot
9.3M
4.6M
-4.6M
-9.3M
uG
-2K
-1K
1K
2K
Oe
File BHPS15C1.dat
Jrs/Js 0.184
Hc 98.794

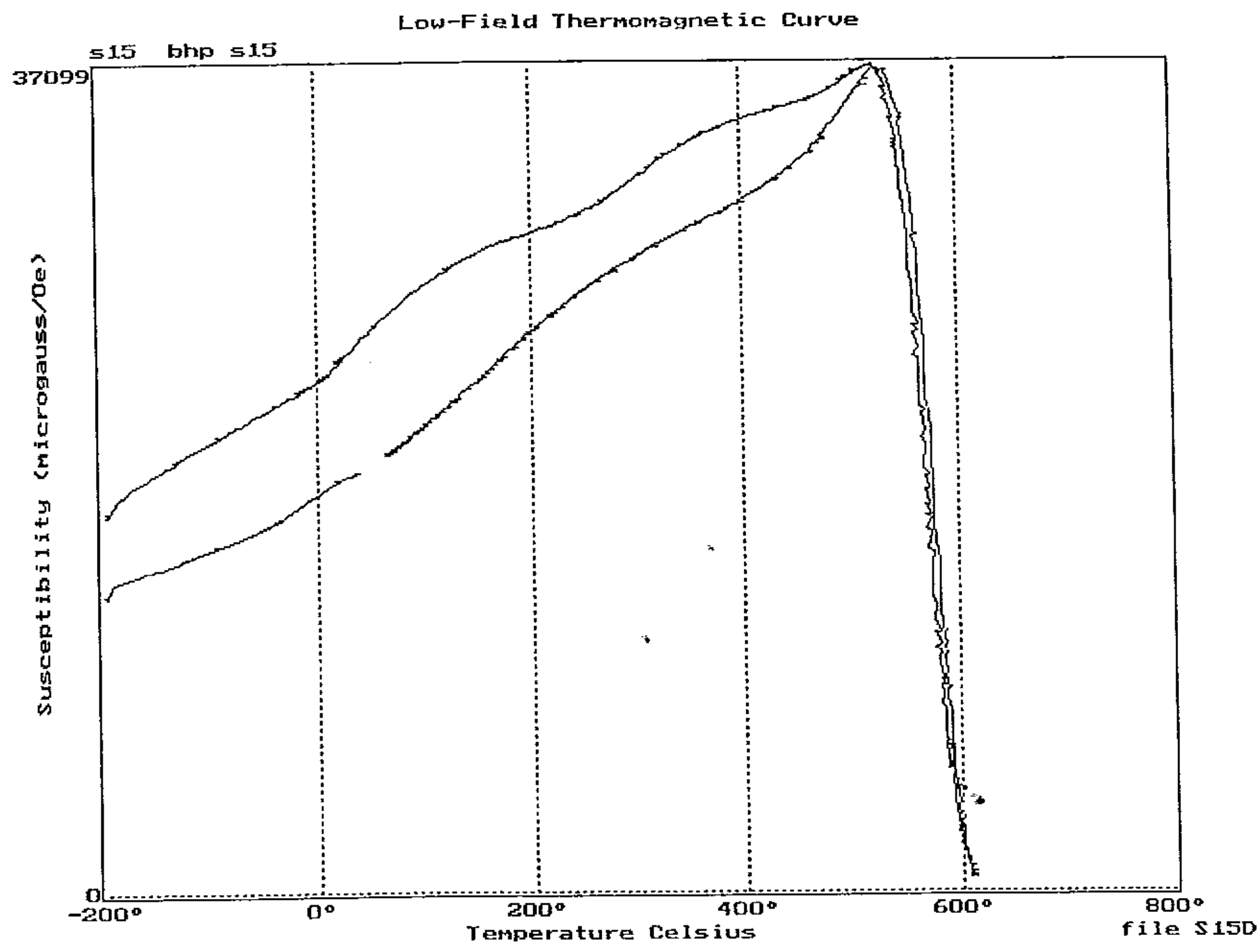
Low-Field Thermomagnetic Curve
s15 bhp s15
37099
0
Susceptibility (microgauss/Oe)
-200°
0°
200°
400°
600°
800°
Temperature Celsius
file S15D

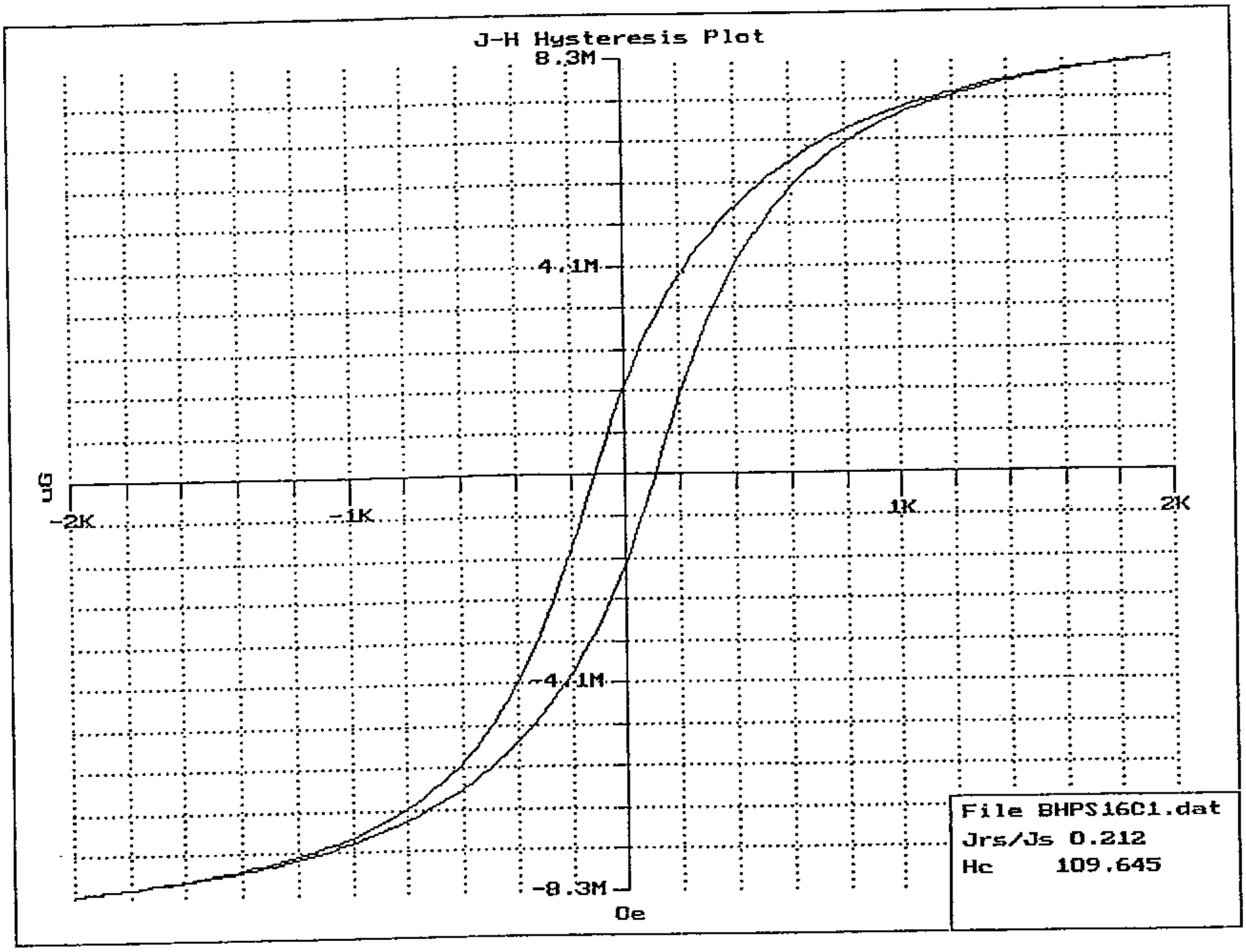
J-H Hysteresis Plot
8.3M
4.1M
uG
-2K
-1K
1K
2K
-4.1M
-8.3M
Oe
File BHPS16C1.dat
Jrs/Js 0.212
Hc 109.645

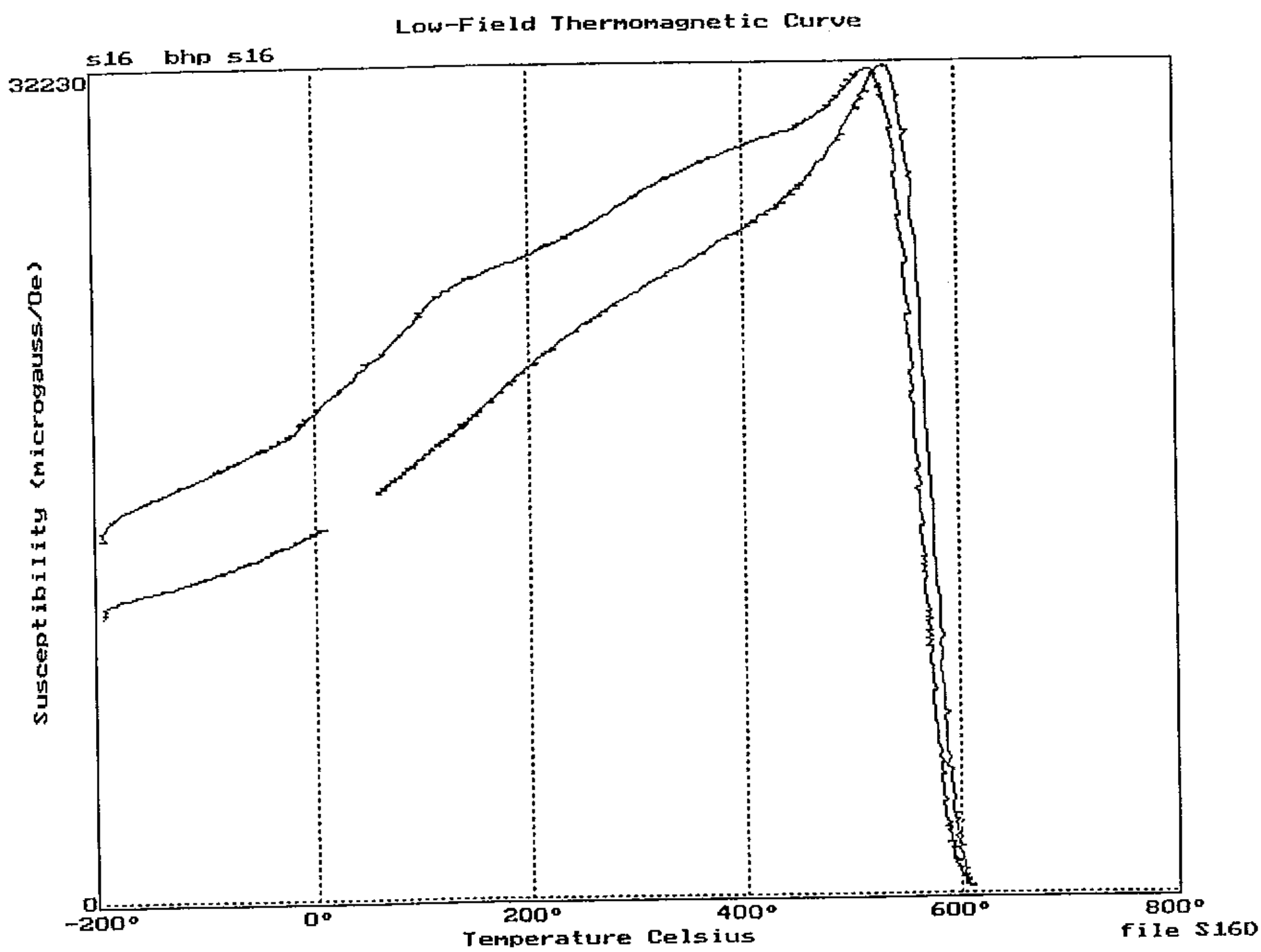
Low-Field Thermomagnetic Curve
s16 bhp s16
32230
Susceptibility (microgauss/Oe)
0
-200°
0°
200°
400°
600°
800°
Temperature Celsius
file S16D

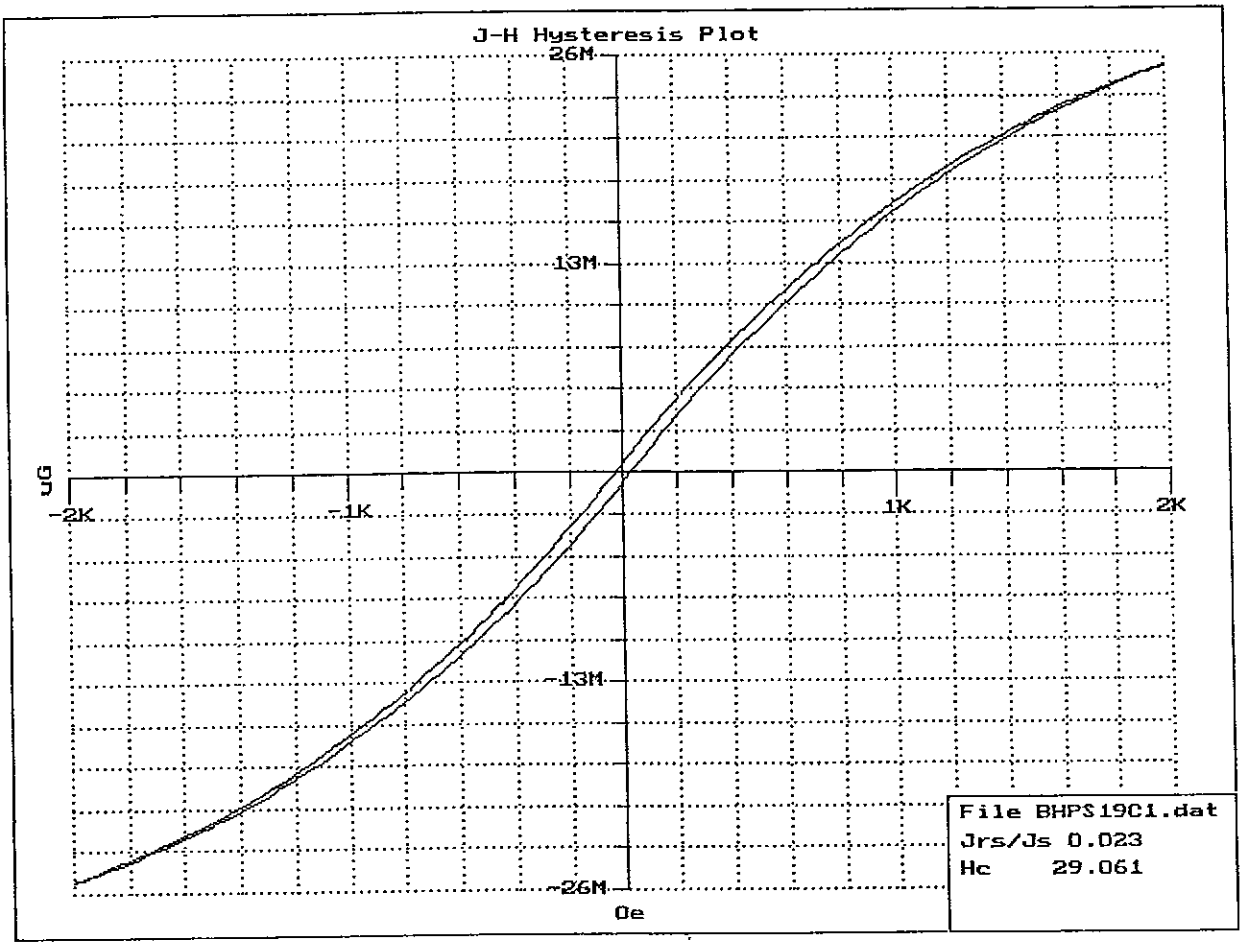
J-H Hysteresis Plot
26M
13M
-13M
-26M
uG
-2K
-1K
1K
2K
Oe
File BHPS19C1.dat
Jrs/Js 0.023
Hc 29.061

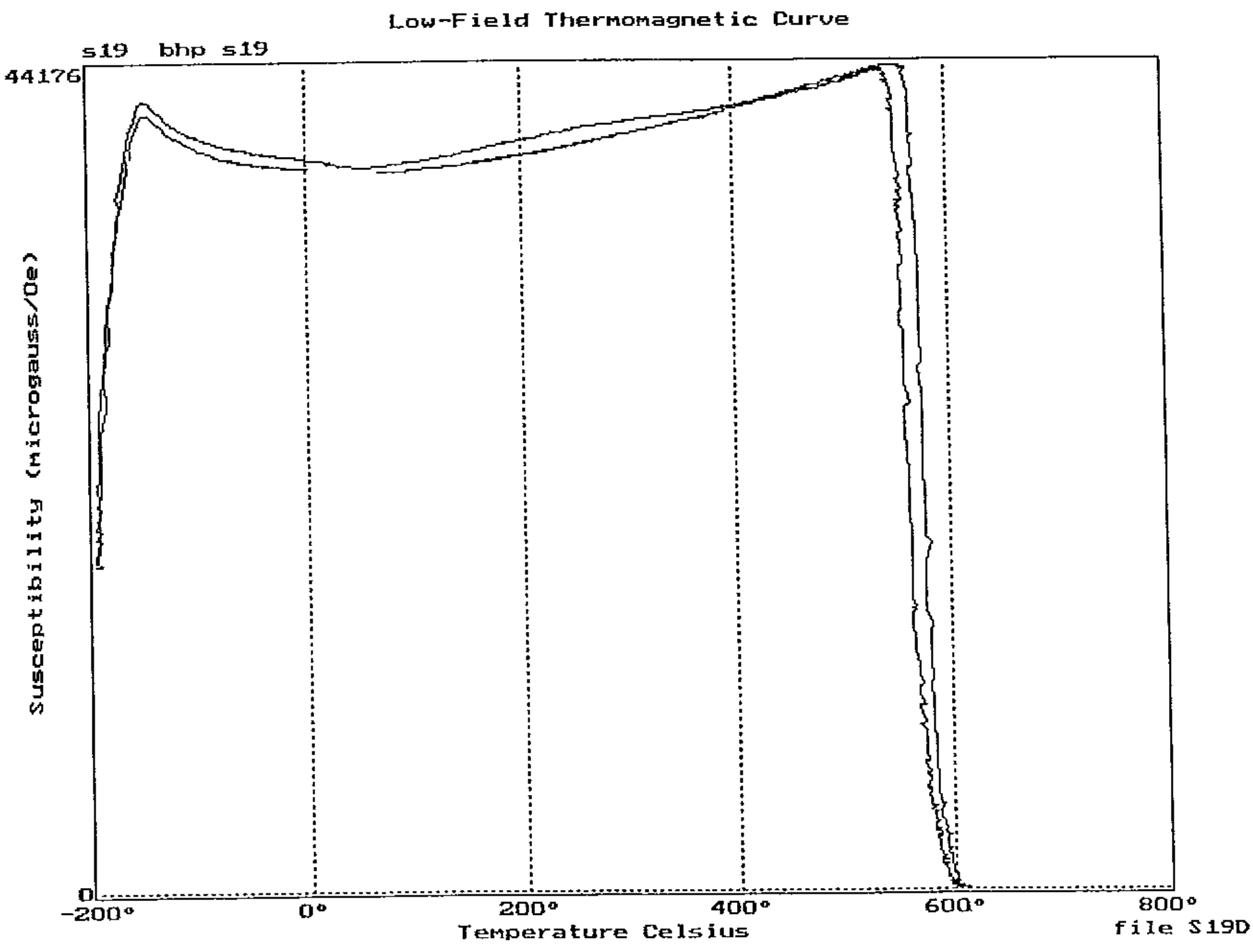
Low-Field Thermomagnetic Curve
s19 bhp s19
44176
0
Susceptibility (microgauss/Oe)
-200°
0°
200°
400°
600°
800°
Temperature Celsius
file S19D

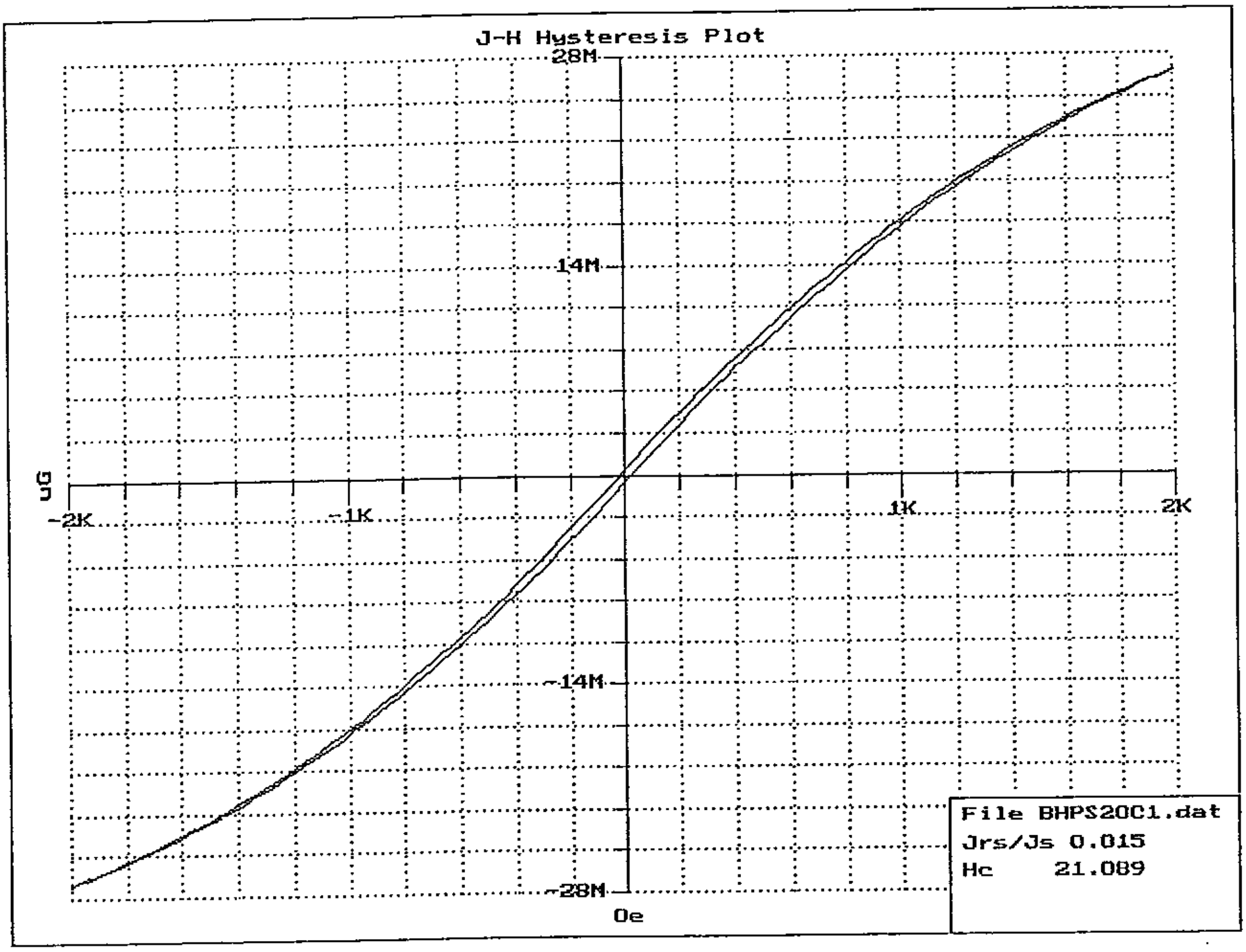
J-H Hysteresis Plot
28M
14M
-14M
-28M
uG
-2K
-1K
1K
2K
Oe
File BHPS20C1.dat
Jrs/Js 0.015
Hc 21.089

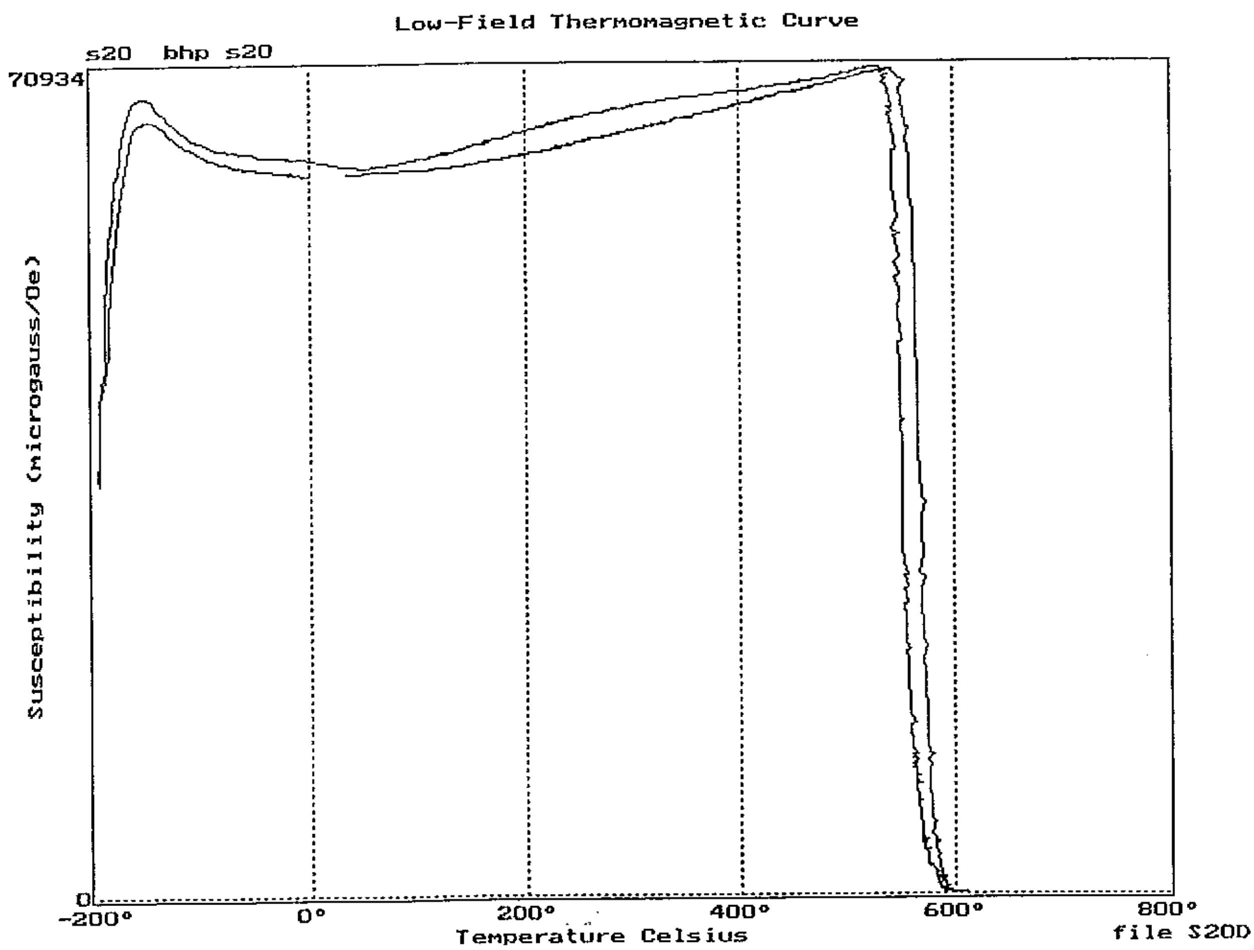
Low-Field Thermomagnetic Curve
s20 bhp s20
70934
0
Susceptibility (microgauss/Oe)
-200°
0°
200°
400°
600°
800°
Temperature Celsius
file S20D

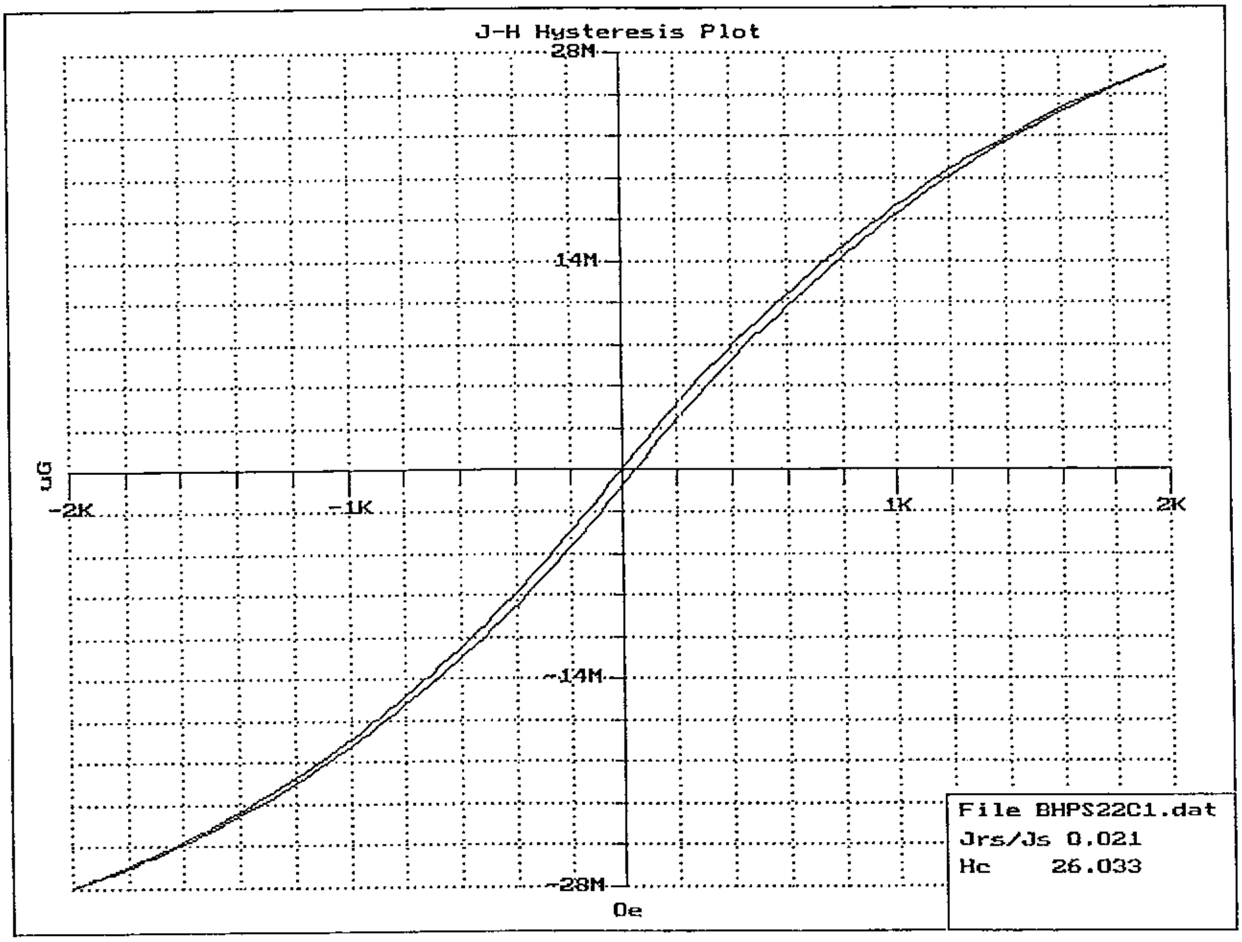
J-H Hysteresis Plot
28M
14M
-14M
-28M
uG
-2K
-1K
1K
2K
Oe
File BHPS22C1.dat
Jrs/Js 0.021
Hc 26.033

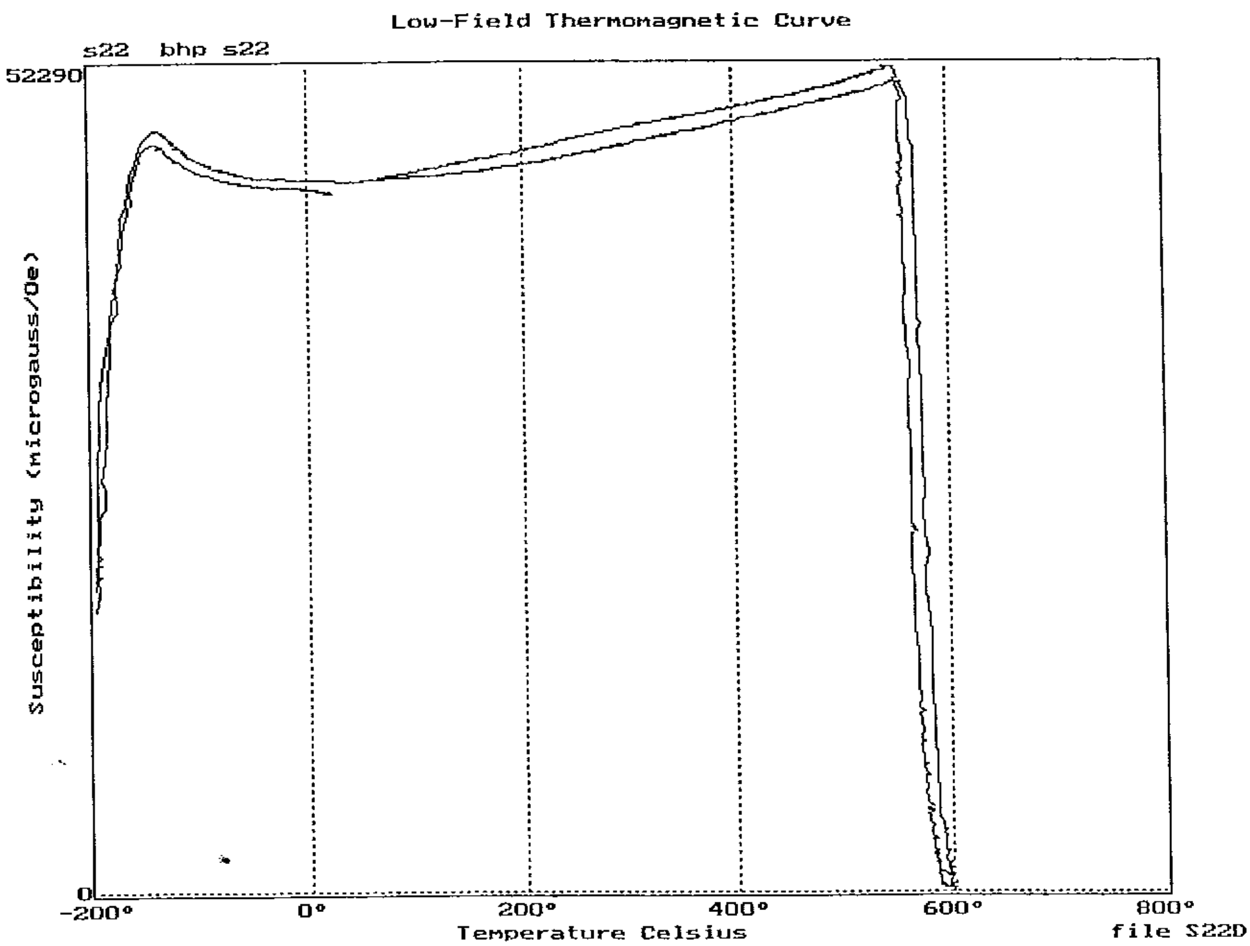
Low-Field Thermomagnetic Curve
s22 bhp s22
52290
0
Susceptibility (microgauss/Oe)
-200°
0°
200°
400°
600°
800°
Temperature Celsius
file S22D

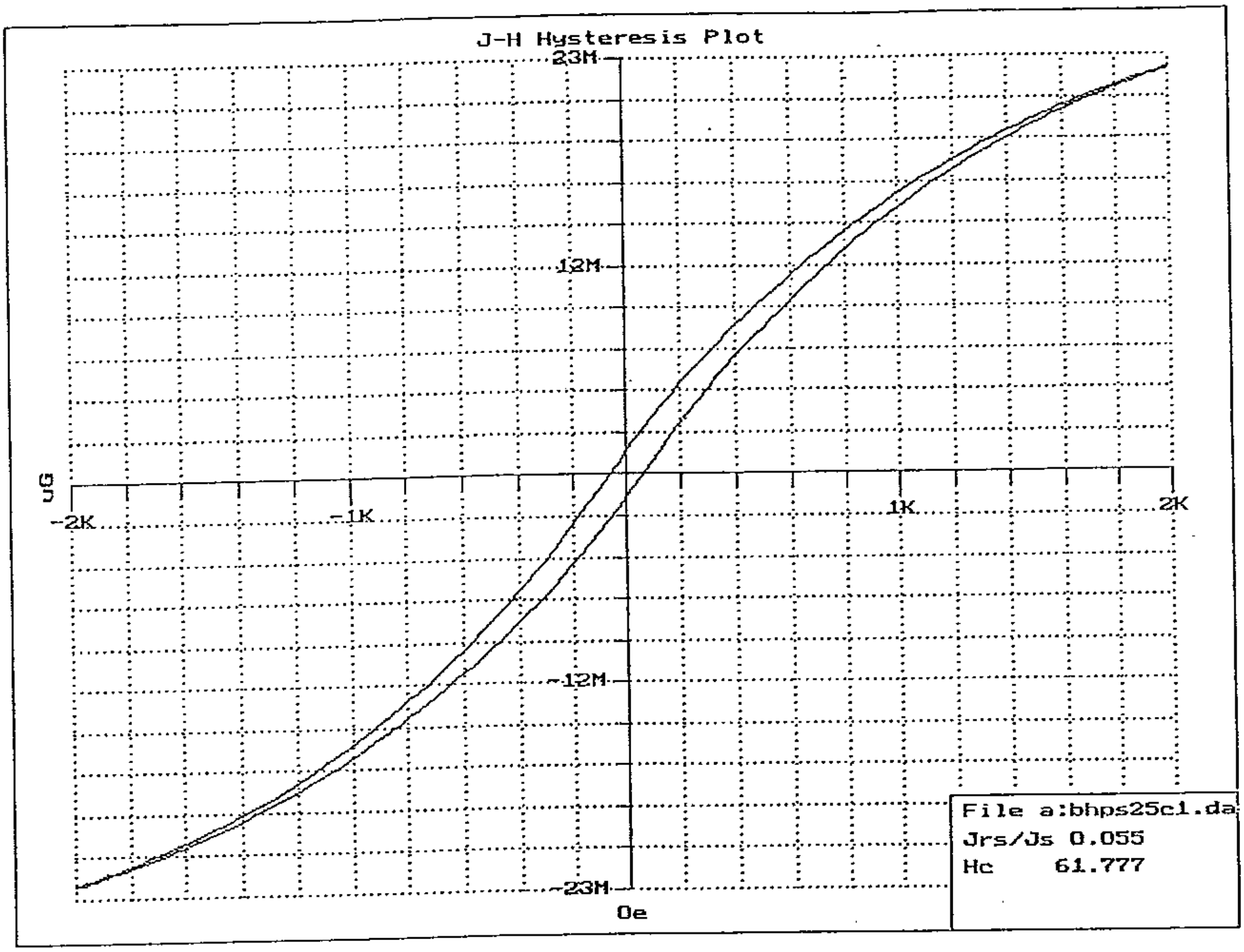
J-H Hysteresis Plot
23M
12M
-12M
-23M
uG
-2K
-1K
1K
2K
Oe
File a:bhps25c1.da
Jrs/Js 0.055
Hc 61.777

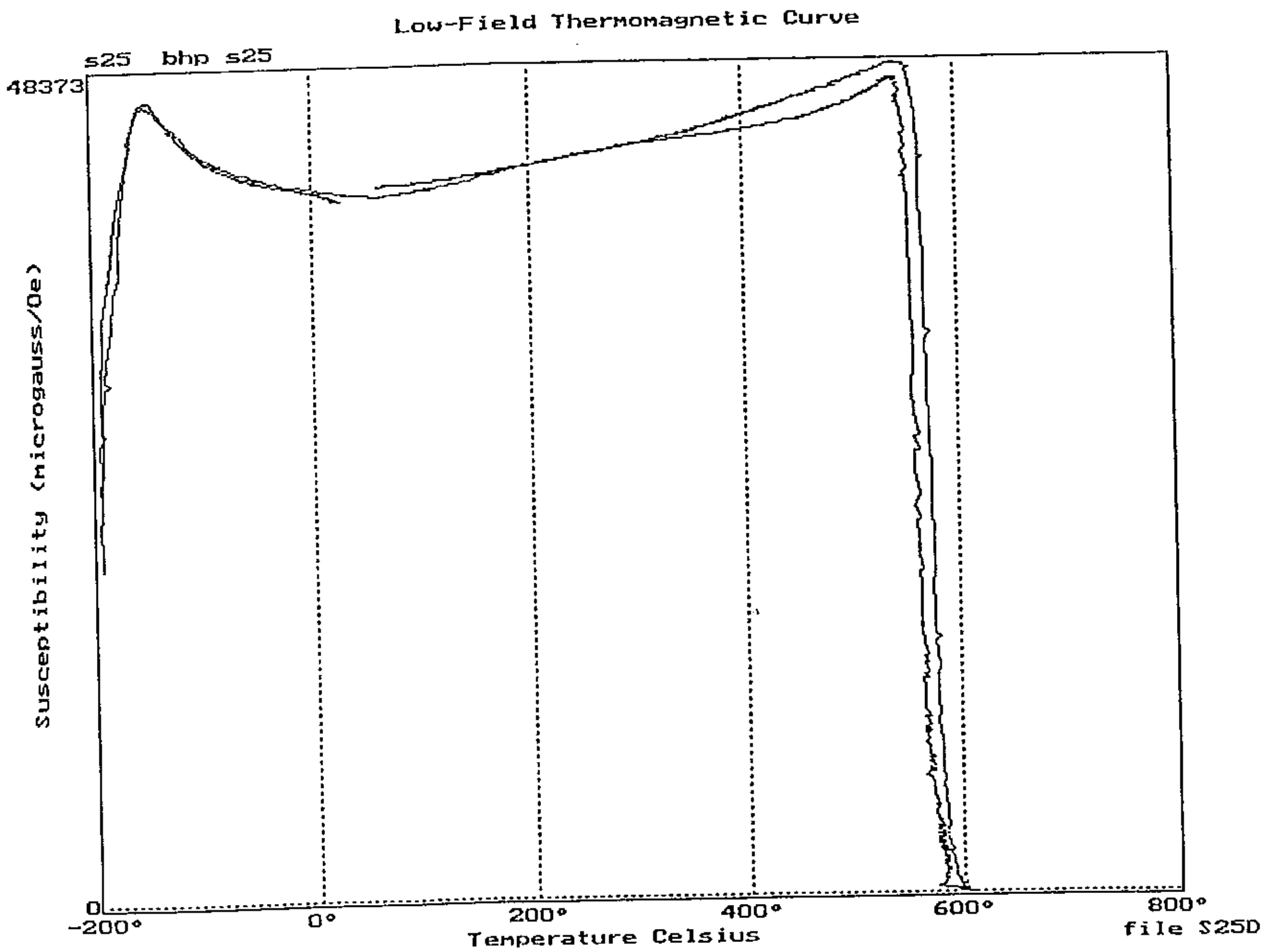
Low-Field Thermomagnetic Curve
s25 bhp s25
48373
0
Susceptibility (microgauss/Oe)
-200°
0°
200°
400°
600°
800°
Temperature Celsius
file S25D

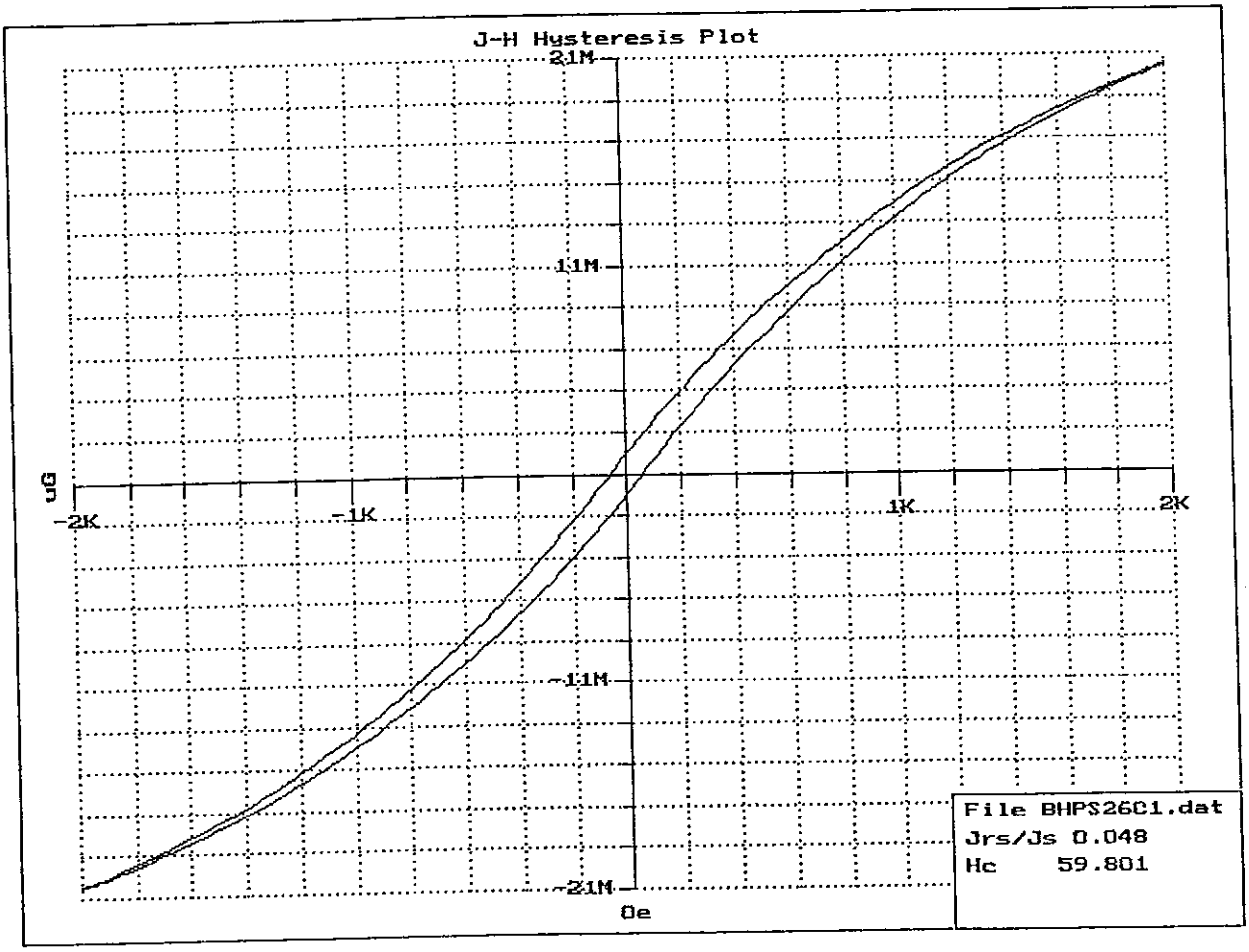
J-H Hysteresis Plot
21M
11M
-11M
-21M
uG
-2K
-1K
1K
2K
Oe
File BHPS26C1.dat
Jrs/Js 0.048
Hc 59.801

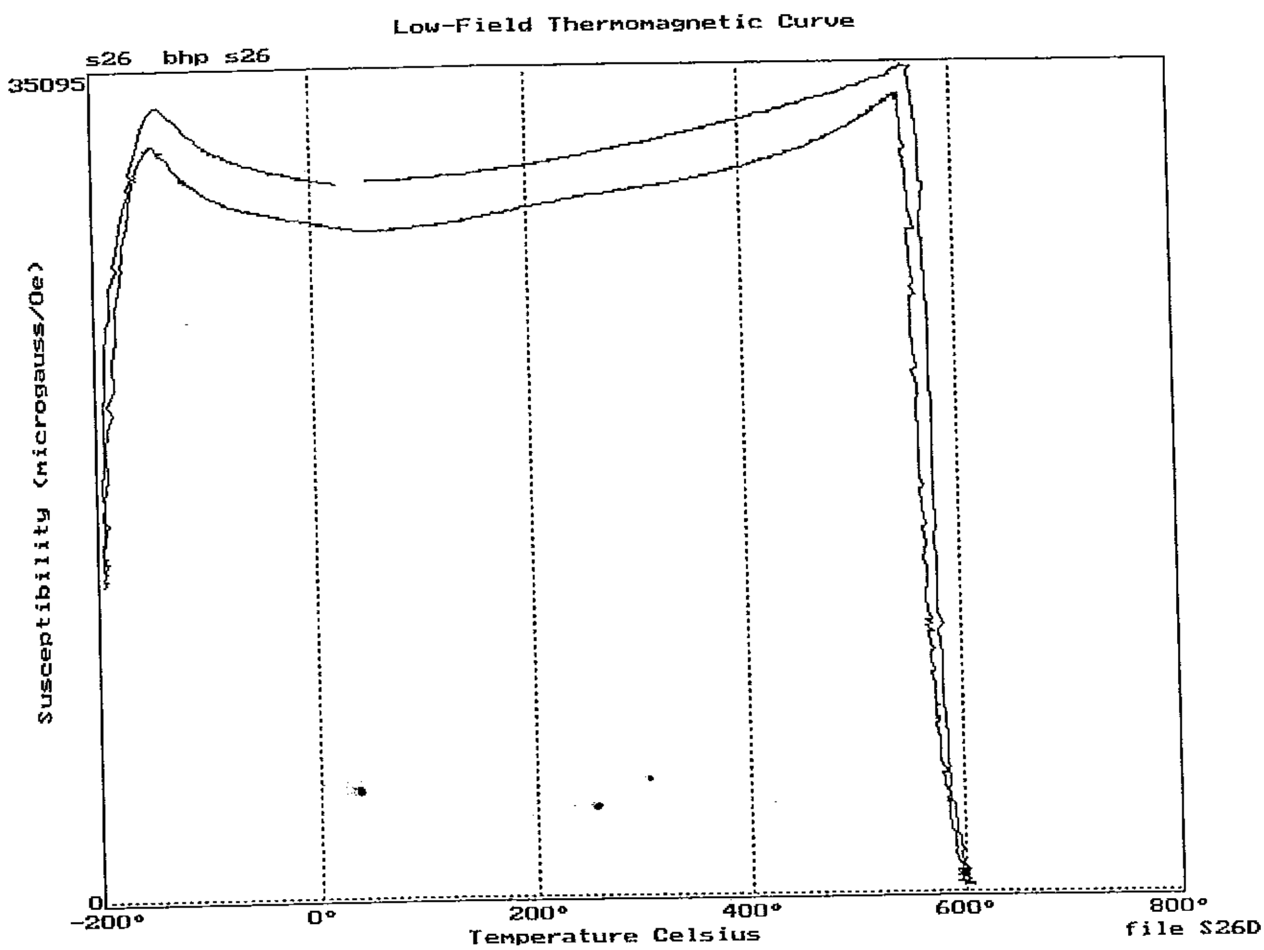
Low-Field Thermomagnetic Curve
s26 bhp s26
35095
0
Susceptibility (microgauss/Oe)
-200°
0°
200°
400°
600°
800°
Temperature Celsius
file S26D

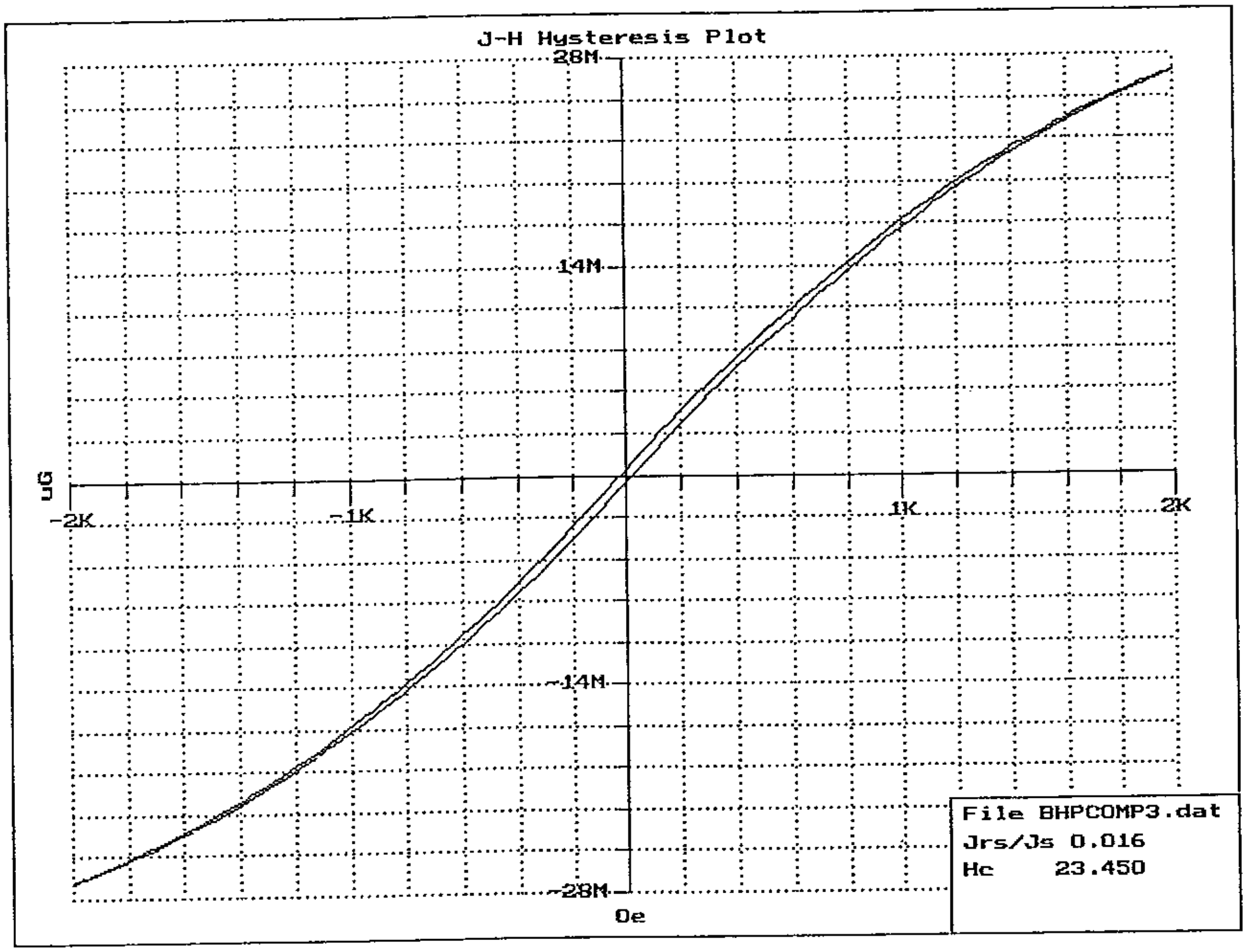
J-H Hysteresis Plot
28M
14M
-14M
-28M
uG
-2K
-1K
1K
2K
Oe
File BHPCOMP3.dat
Jrs/Js 0.016
Hc 23.450

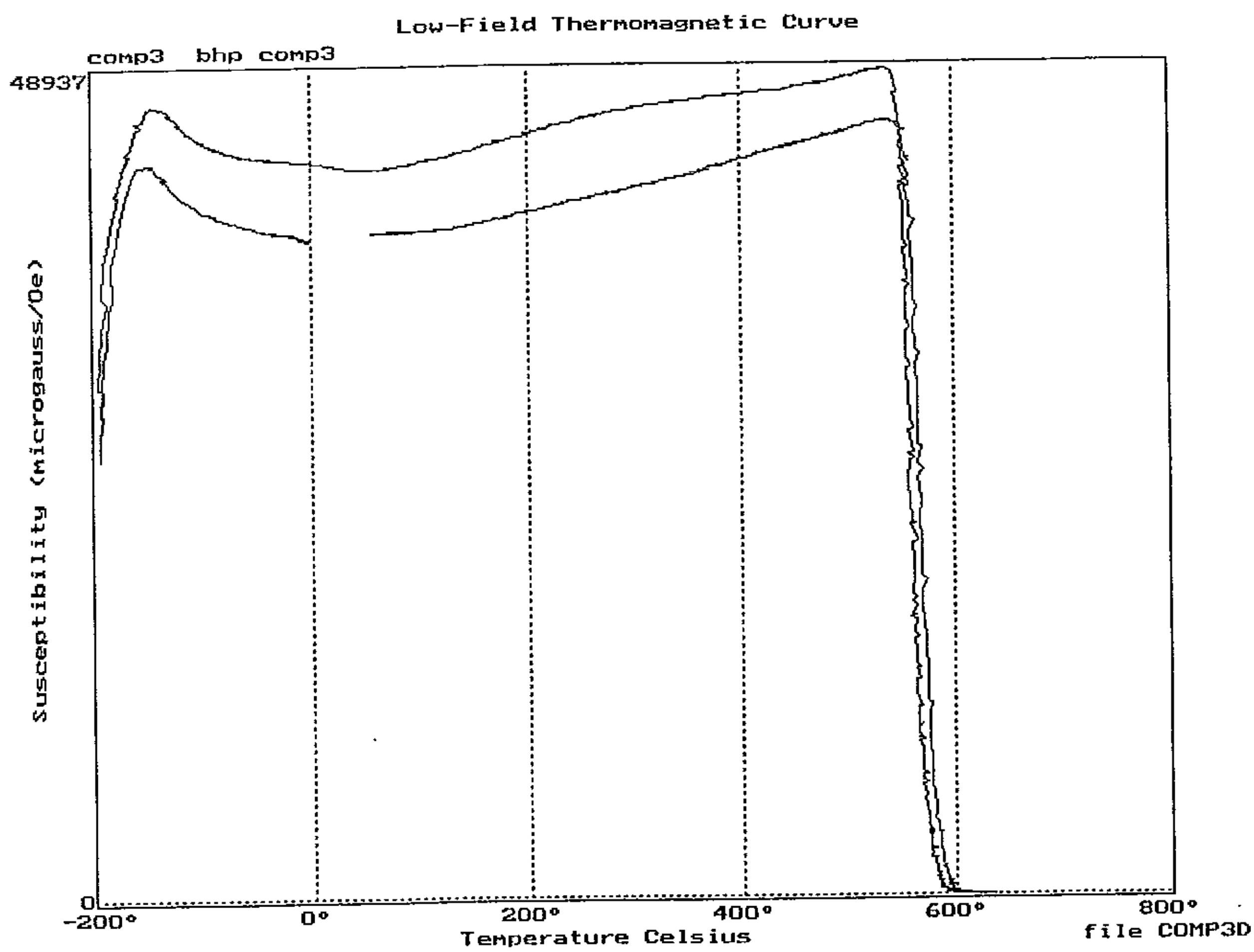
Low-Field Thermomagnetic Curve
comp3 bhp comp3
48937
0
Susceptibility (microgauss/Oe)
-200°
0°
200°
400°
600°
800°
Temperature Celsius
file COMP3D

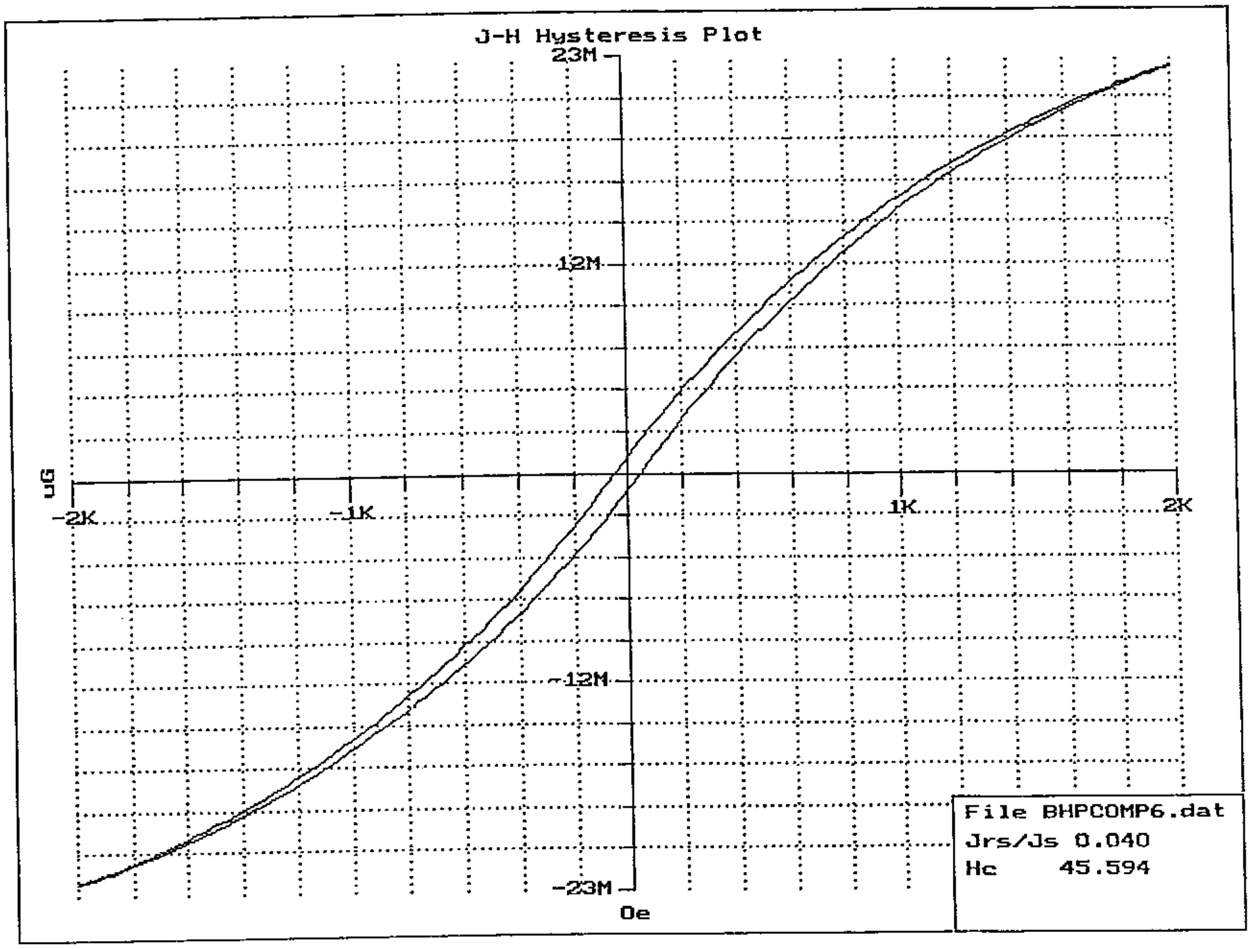
J-H Hysteresis Plot
23M
12M
-12M
-23M
uG
-2K
-1K
1K
2K
Oe
File BHPCOMP6.dat
Jrs/Js 0.040
Hc 45.594

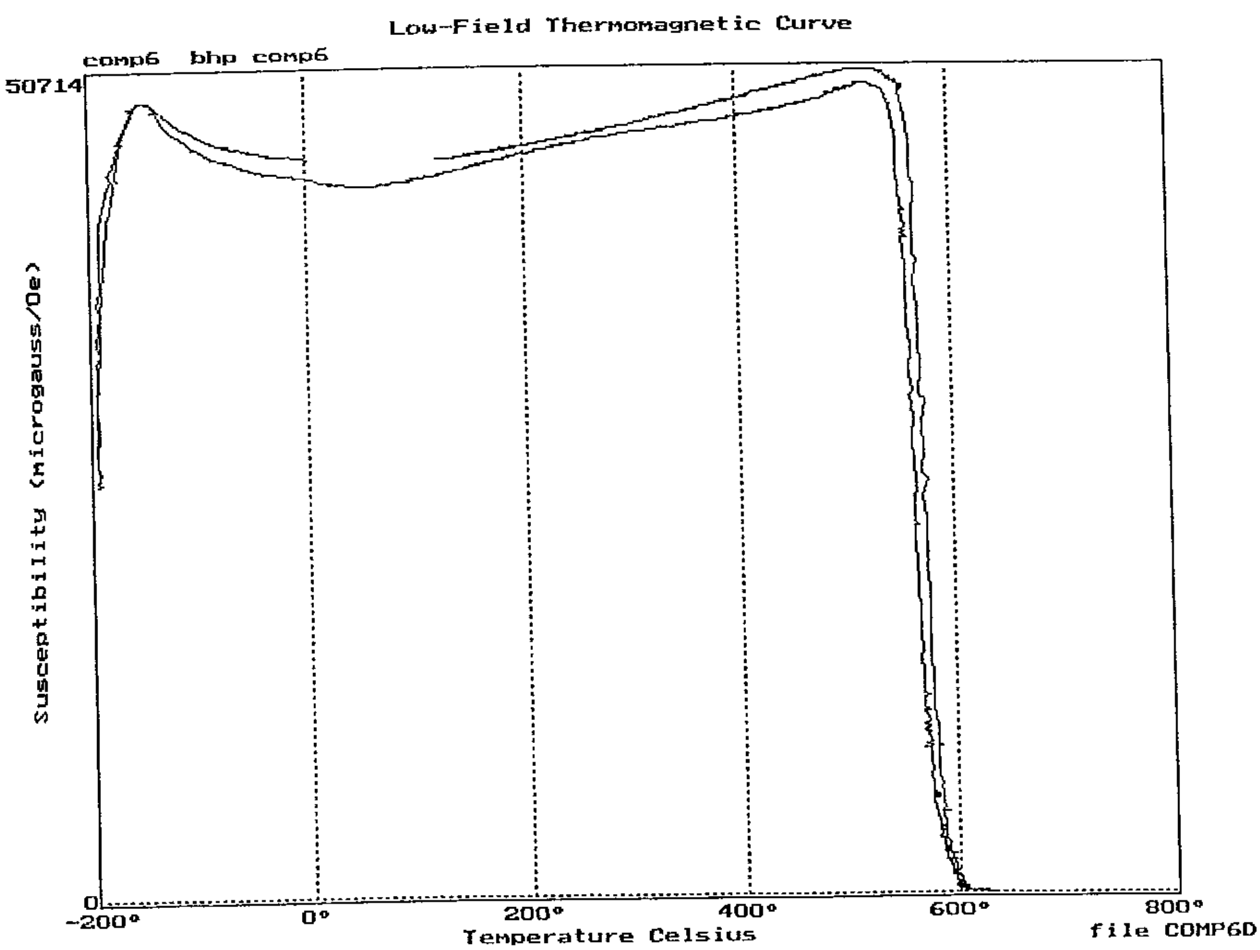
Low-Field Thermomagnetic Curve
comp6 bhp comp6
50714
0
Susceptibility (microgauss/Oe)
-200°
0°
200°
400°
600°
800°
Temperature Celsius
file COMP6D

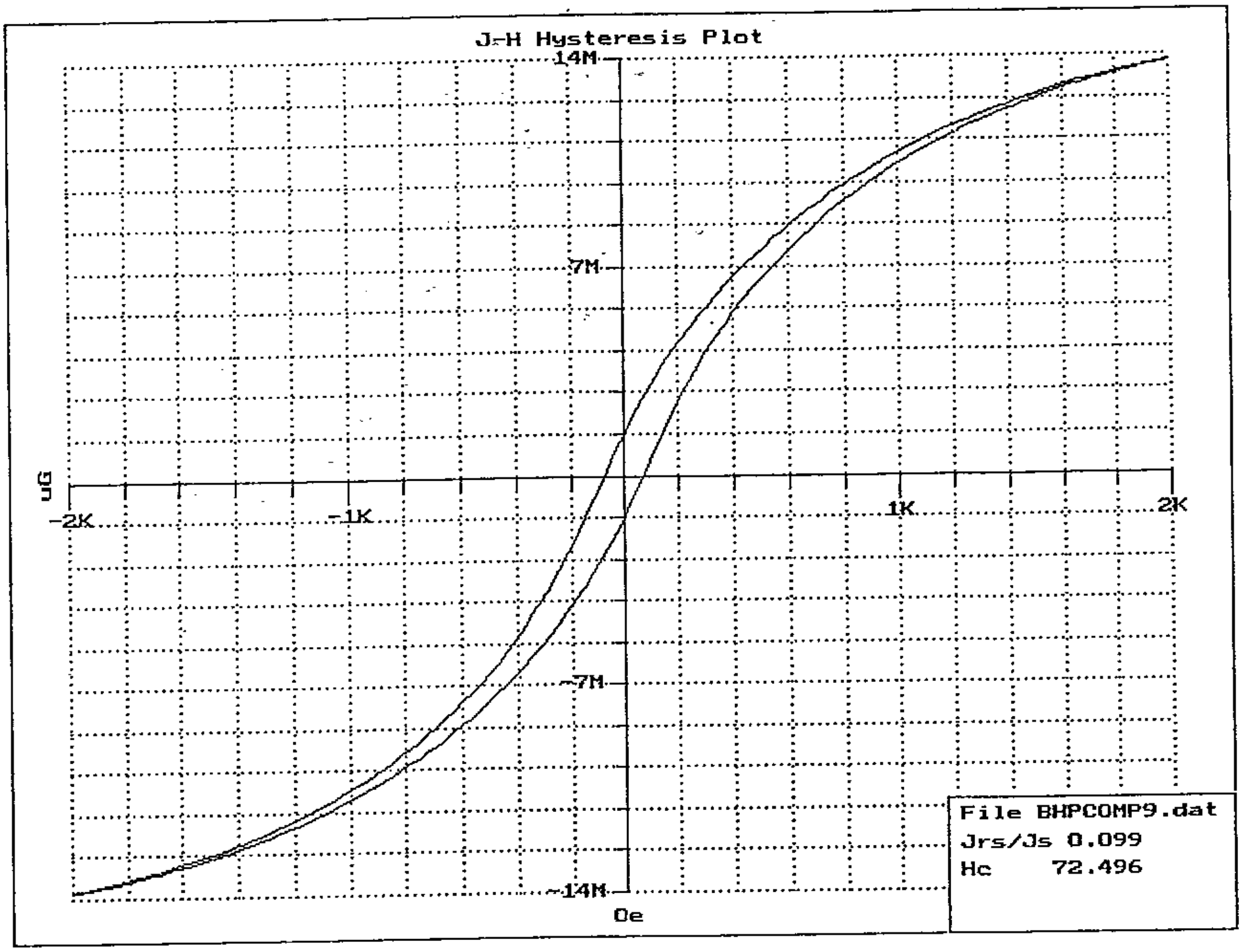
J-H Hysteresis Plot
14M
7M
-7M
-14M
uG
-2K
-1K
1K
2K
Oe
File BHPCOMP9.dat
Jrs/Js 0.099
Hc 72.496

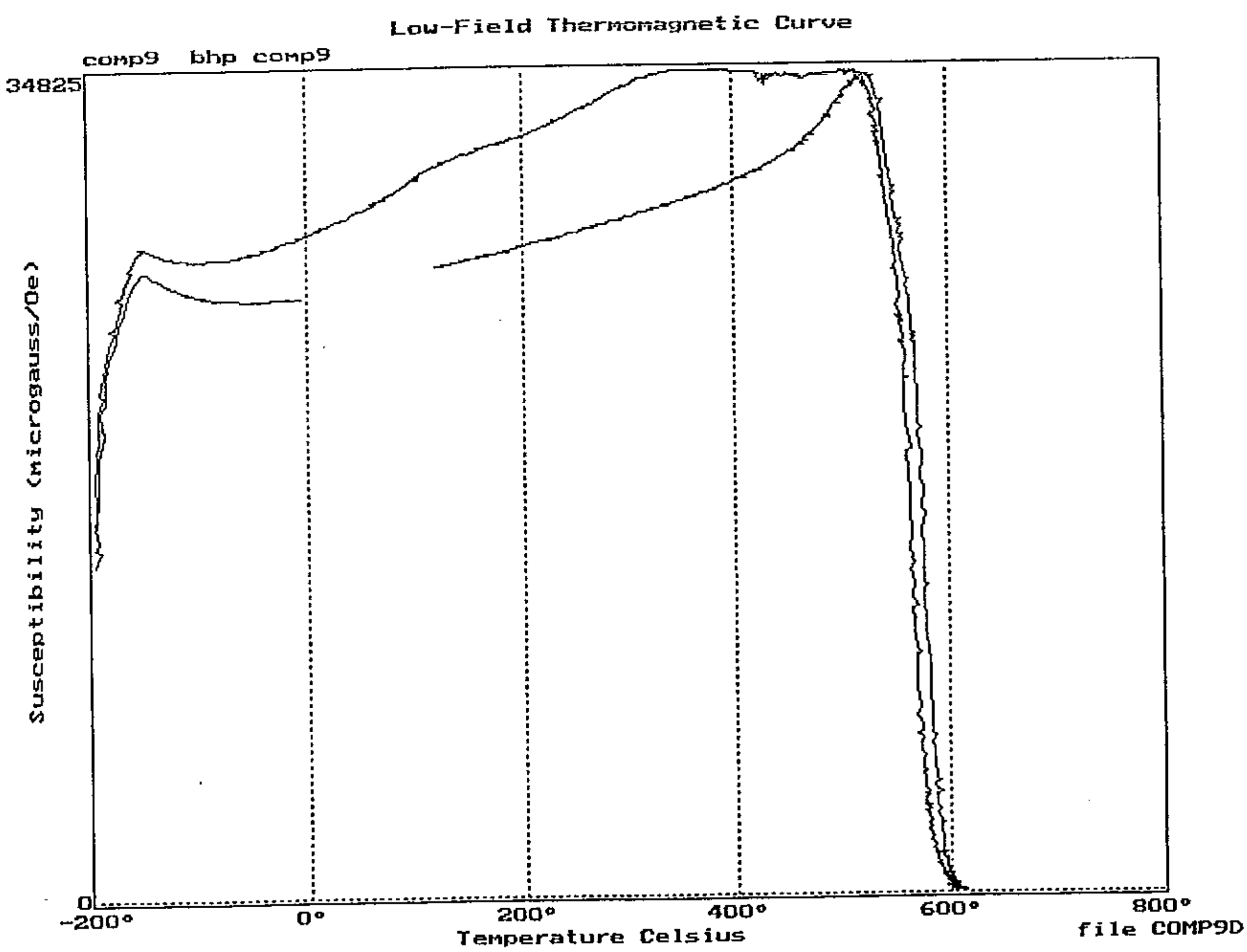
Low-Field Thermomagnetic Curve
comp9 bhp comp9
34825
0
Susceptibility (microgauss/Oe)
-200°
0°
200°
400°
600°
800°
Temperature Celsius
file COMP9D

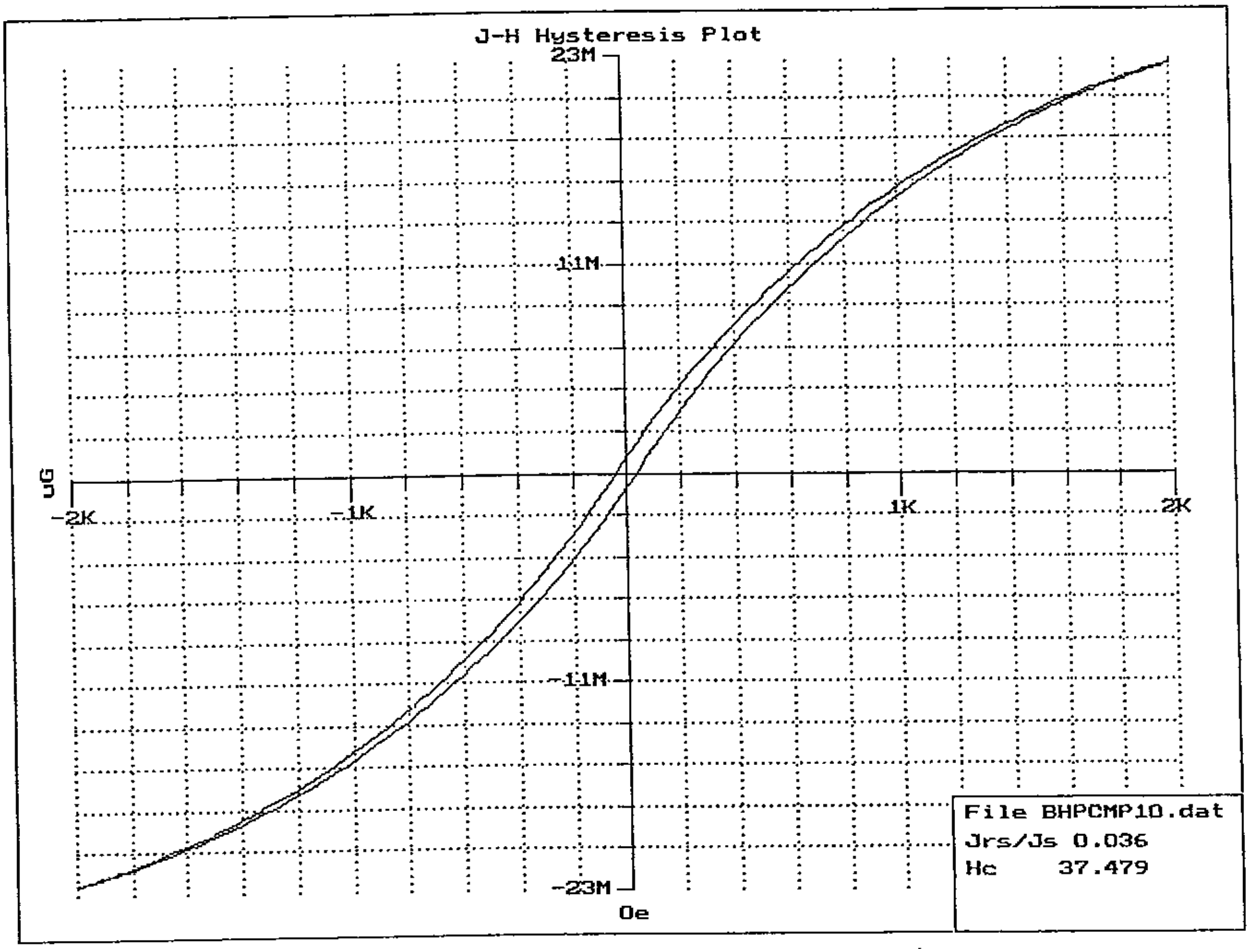
J-H Hysteresis Plot
23M
11M
-11M
-23M
uG
-2K
-1K
1K
2K
Oe
File BHPCMP10.dat
Jrs/Js 0.036
Hc 37.479

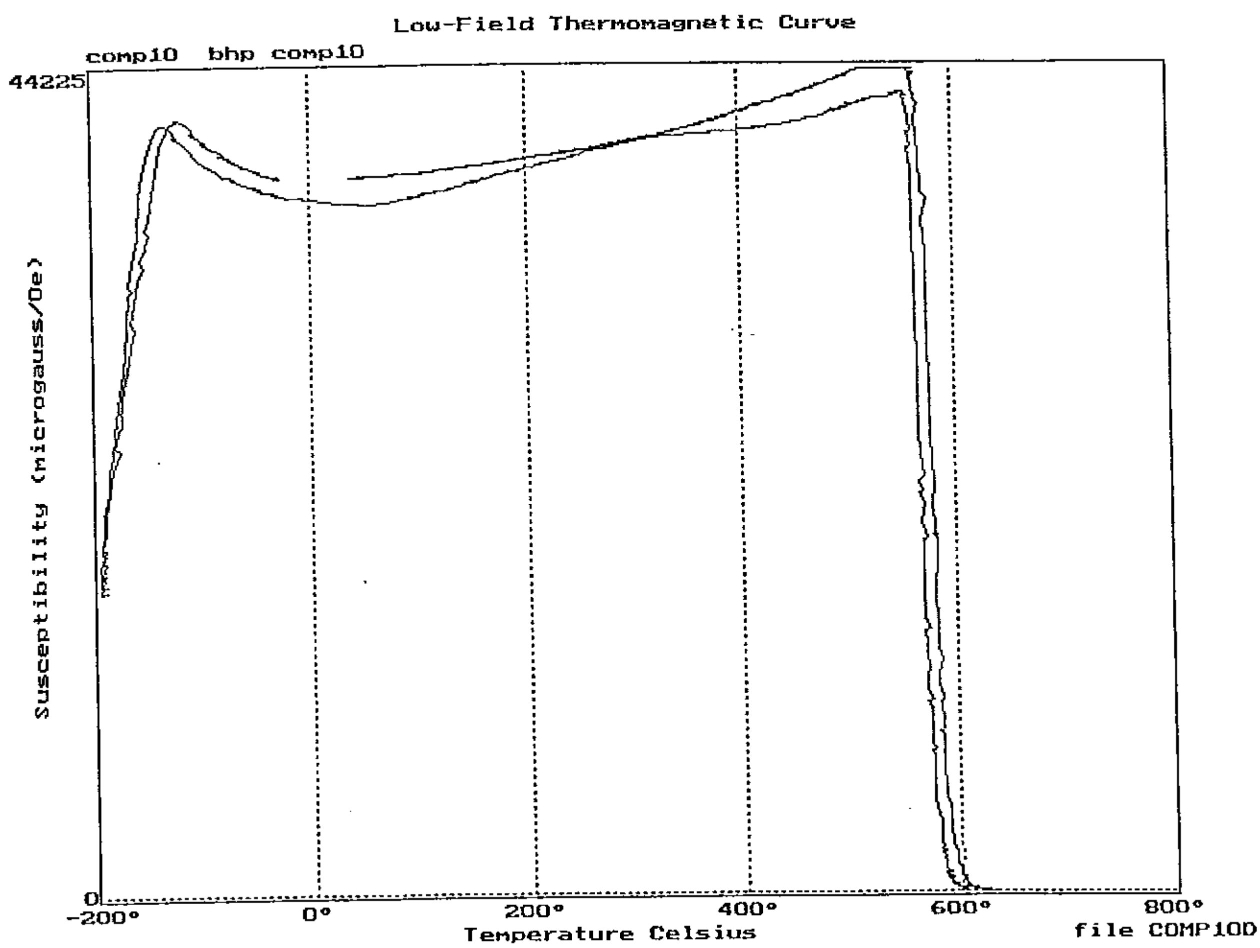
Low-Field Thermomagnetic Curve
comp10 bhp comp10
44225
0
Susceptibility (microgauss/Oe)
-200°
0°
200°
400°
600°
800°
Temperature Celsius
file COMP10D

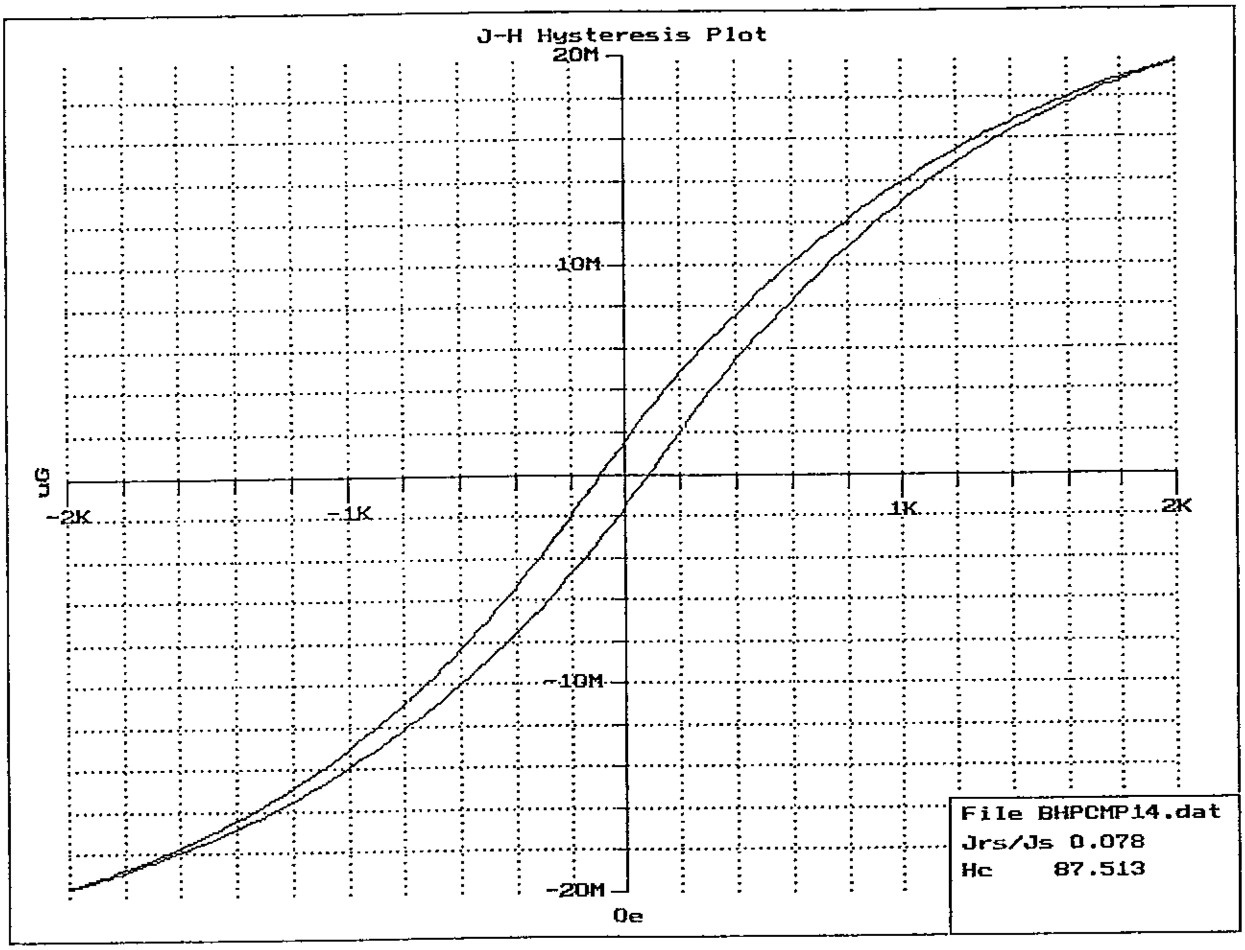
J-H Hysteresis Plot
20M
10M
-10M
-20M
uG
-2K
-1K
1K
2K
Oe
File BHPCMP14.dat
Jrs/Js 0.078
Hc 87.513

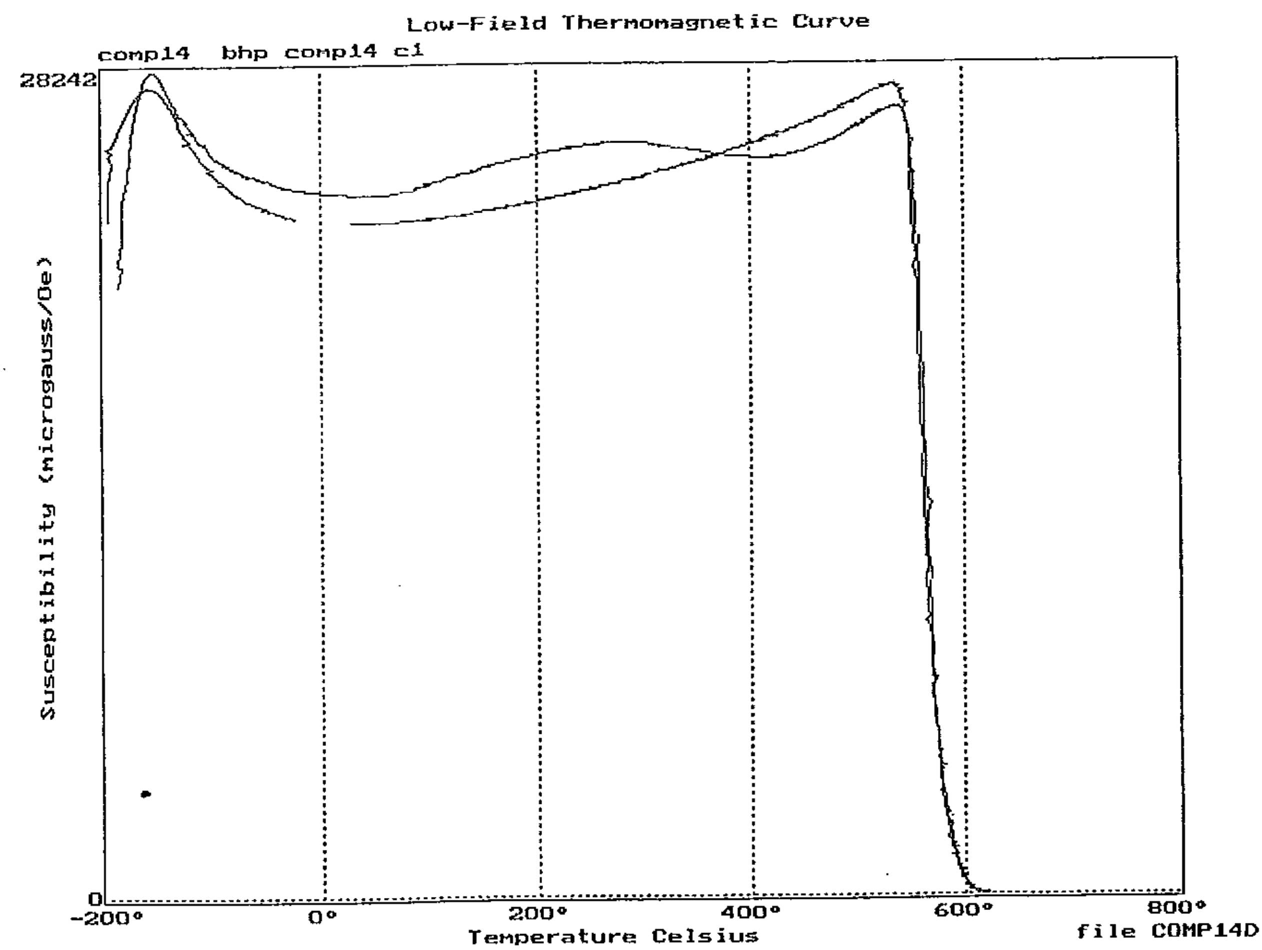
Low-Field Thermomagnetic Curve
comp14 bhp comp14 c1
28242
0
Susceptibility (microgauss/Oe)
-200°
0°
200°
400°
600°
800°
Temperature Celsius
file COMP14D

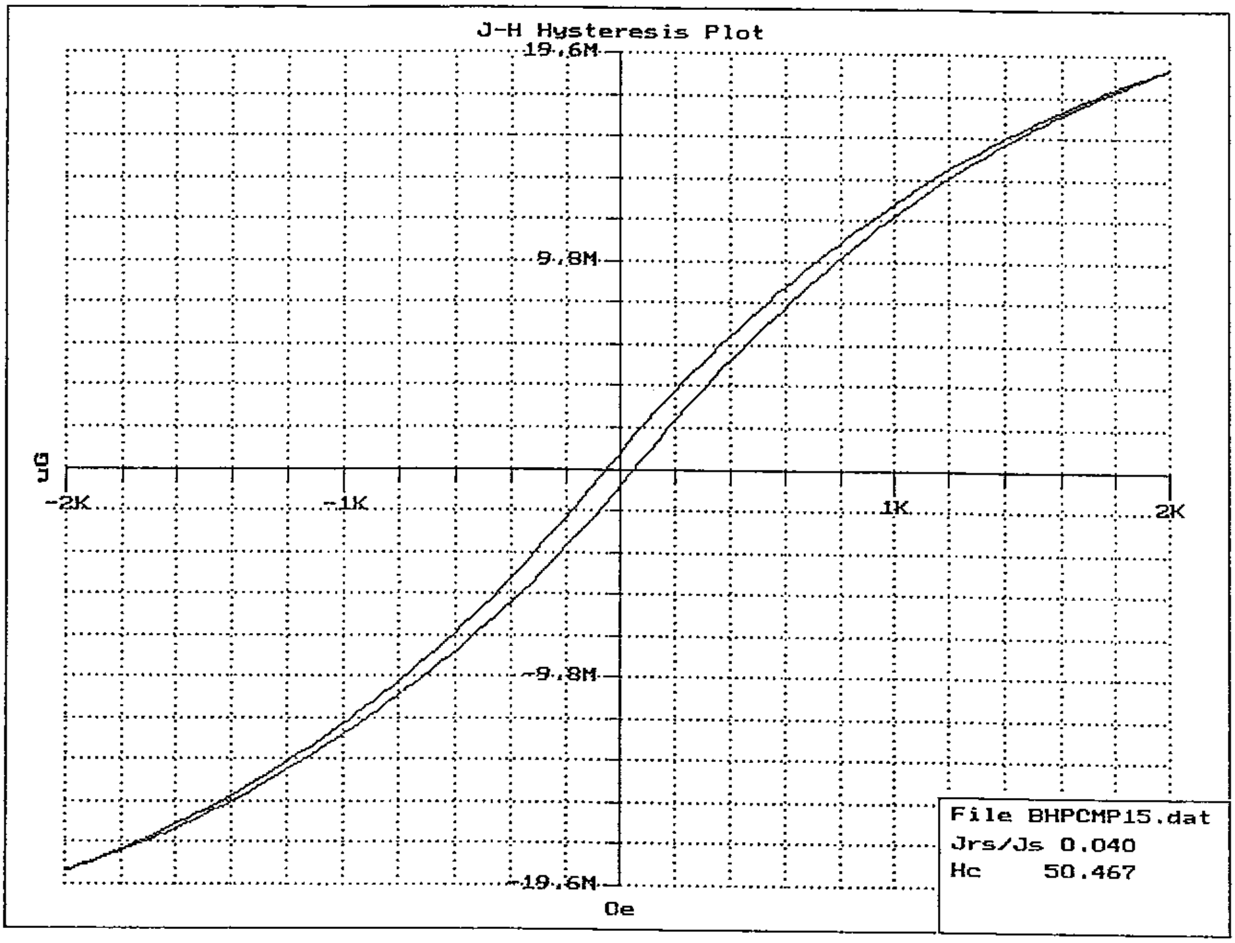
J-H Hysteresis Plot
19.6M
9.8M
-9.8M
-19.6M
uG
-2K
-1K
1K
2K
Oe
File BHPCMP15.dat
Jrs/Js 0.040
Hc 50.467

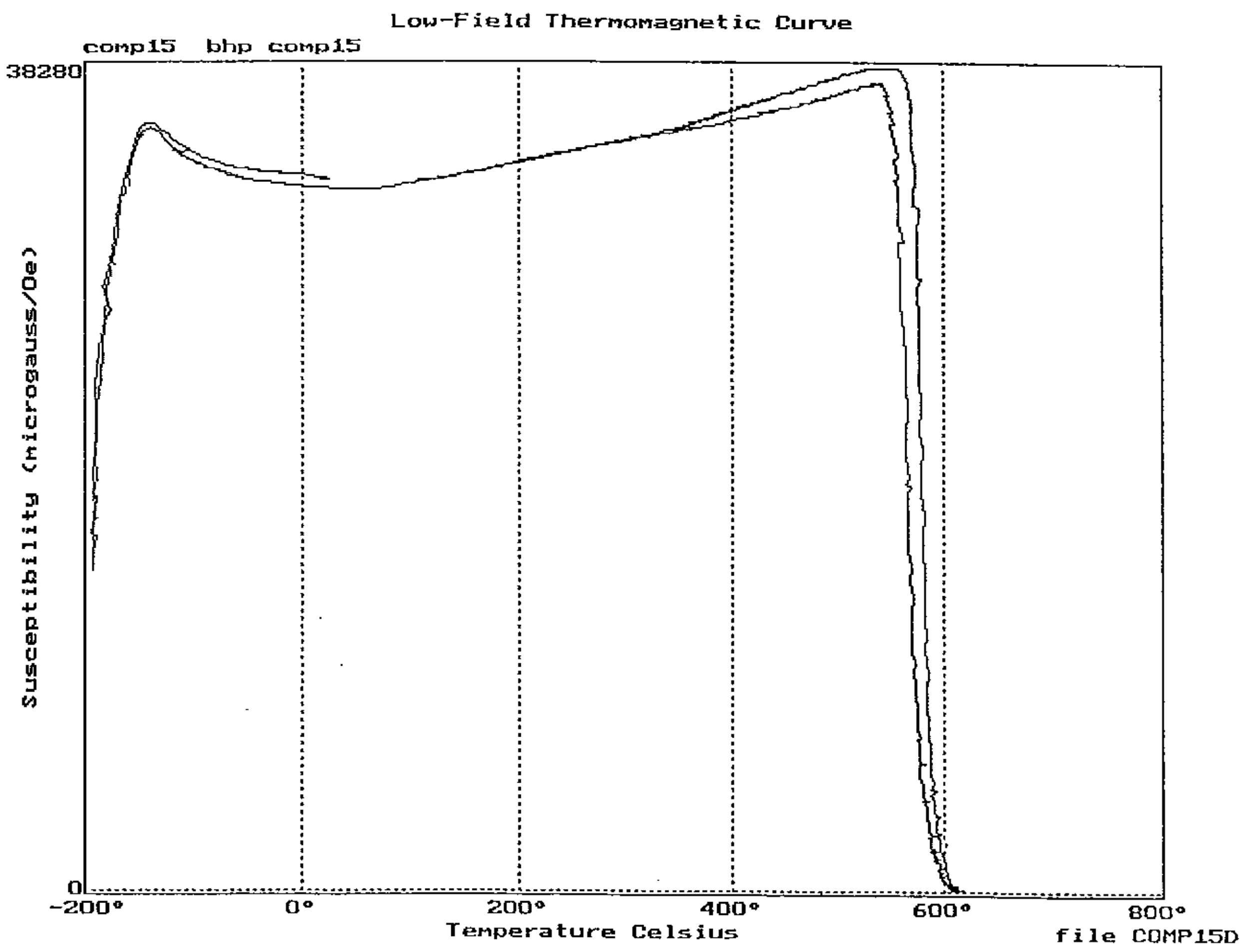
Low-Field Thermomagnetic Curve
comp15 bhp comp15
38280
0
Susceptibility (microgauss/Oe)
-200°
0°
200°
400°
600°
800°
Temperature Celsius
file COMP15D

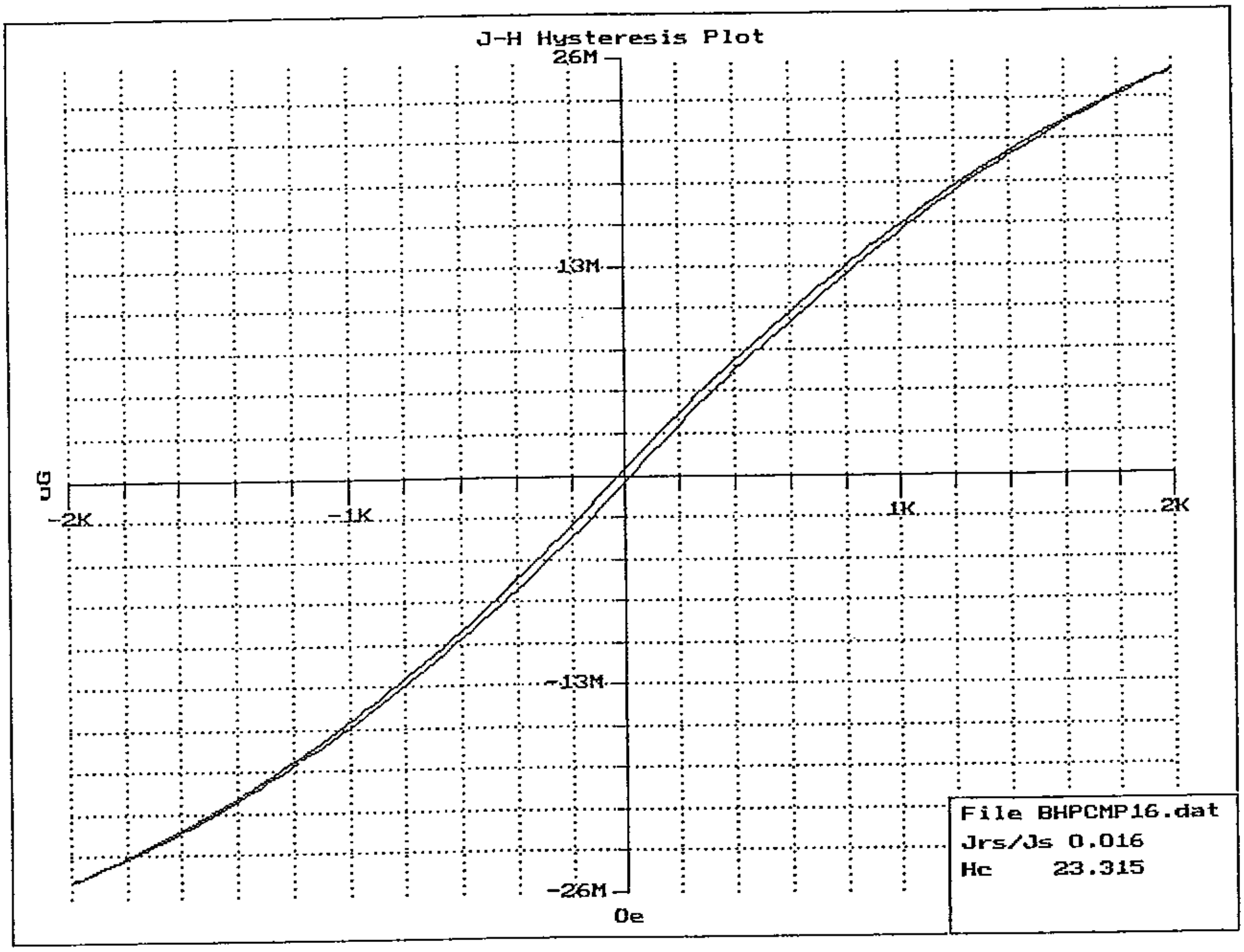
J-H Hysteresis Plot
26M
13M
-13M
-26M
uG
-2K
-1K
1K
2K
Oe
File BHPCMP16.dat
Jrs/Js 0.016
Hc 23.315

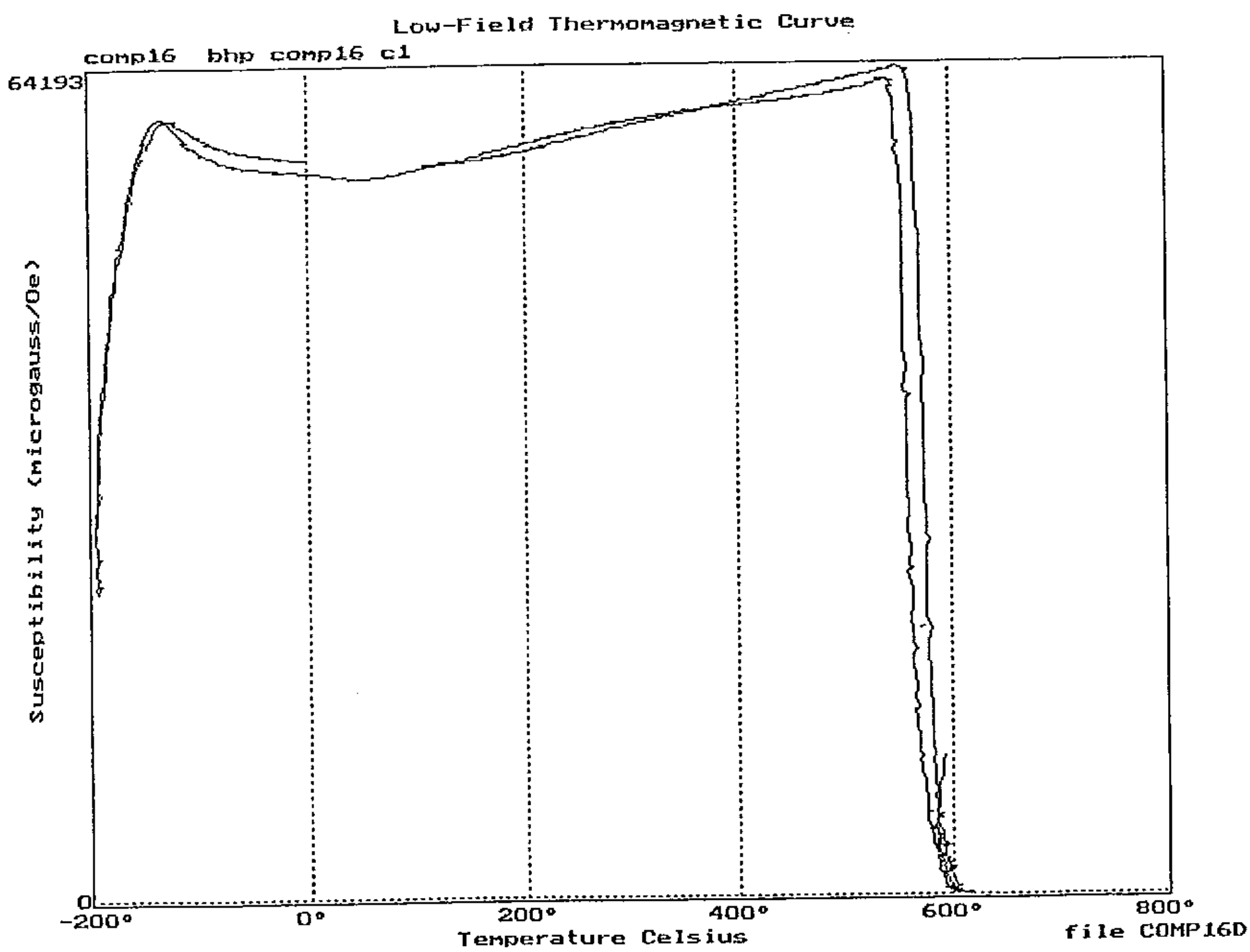
Low-Field Thermomagnetic Curve
comp16 bhp comp16 c1
64193
0
Susceptibility (microgauss/Oe)
-200°
0°
200°
400°
600°
800°
Temperature Celsius
file COMP16D

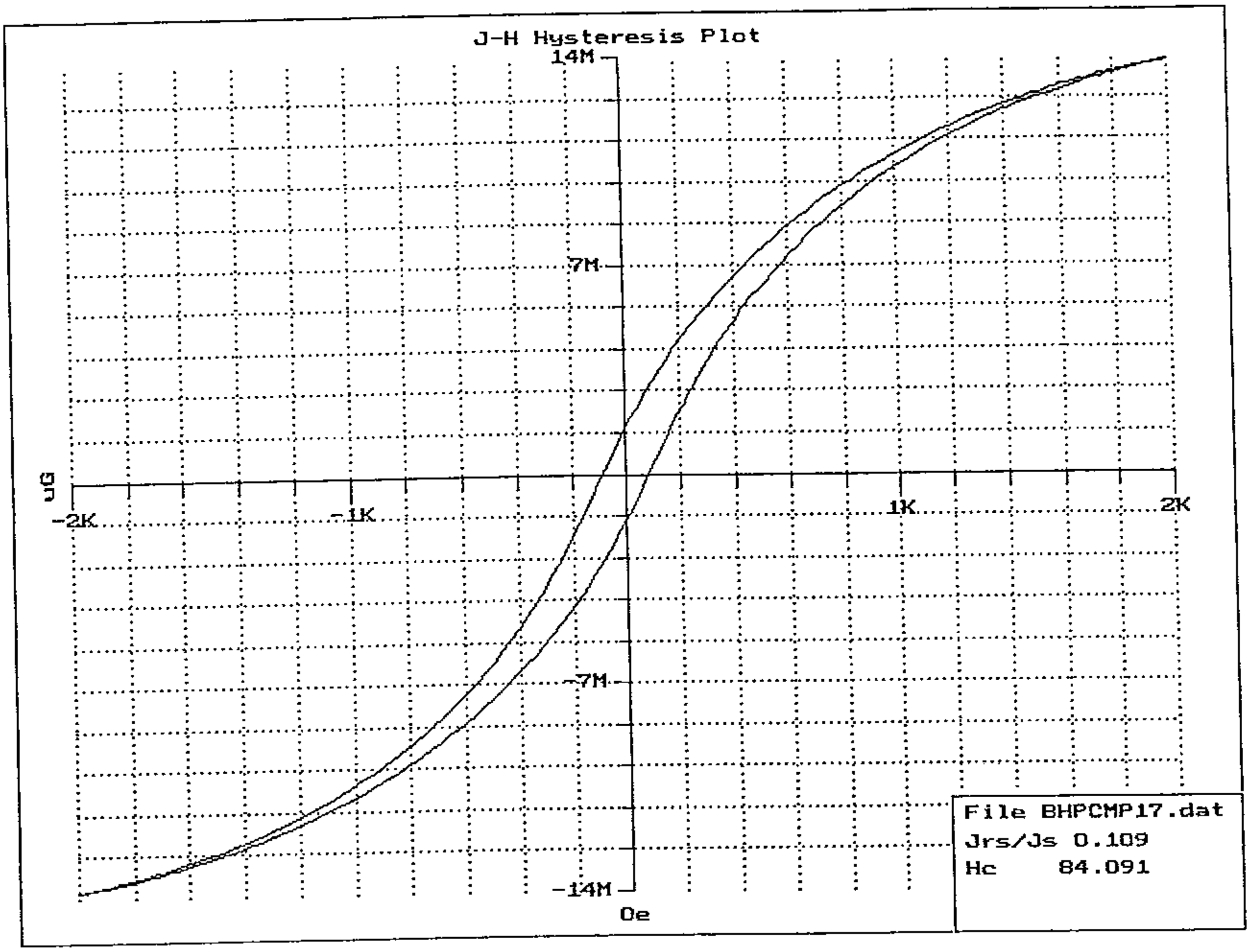
J-H Hysteresis Plot
14M
7M
-7M
-14M
uG
-2K
-1K
1K
2K
Oe
File BHPCMP17.dat
Jrs/Js 0.109
Hc 84.091

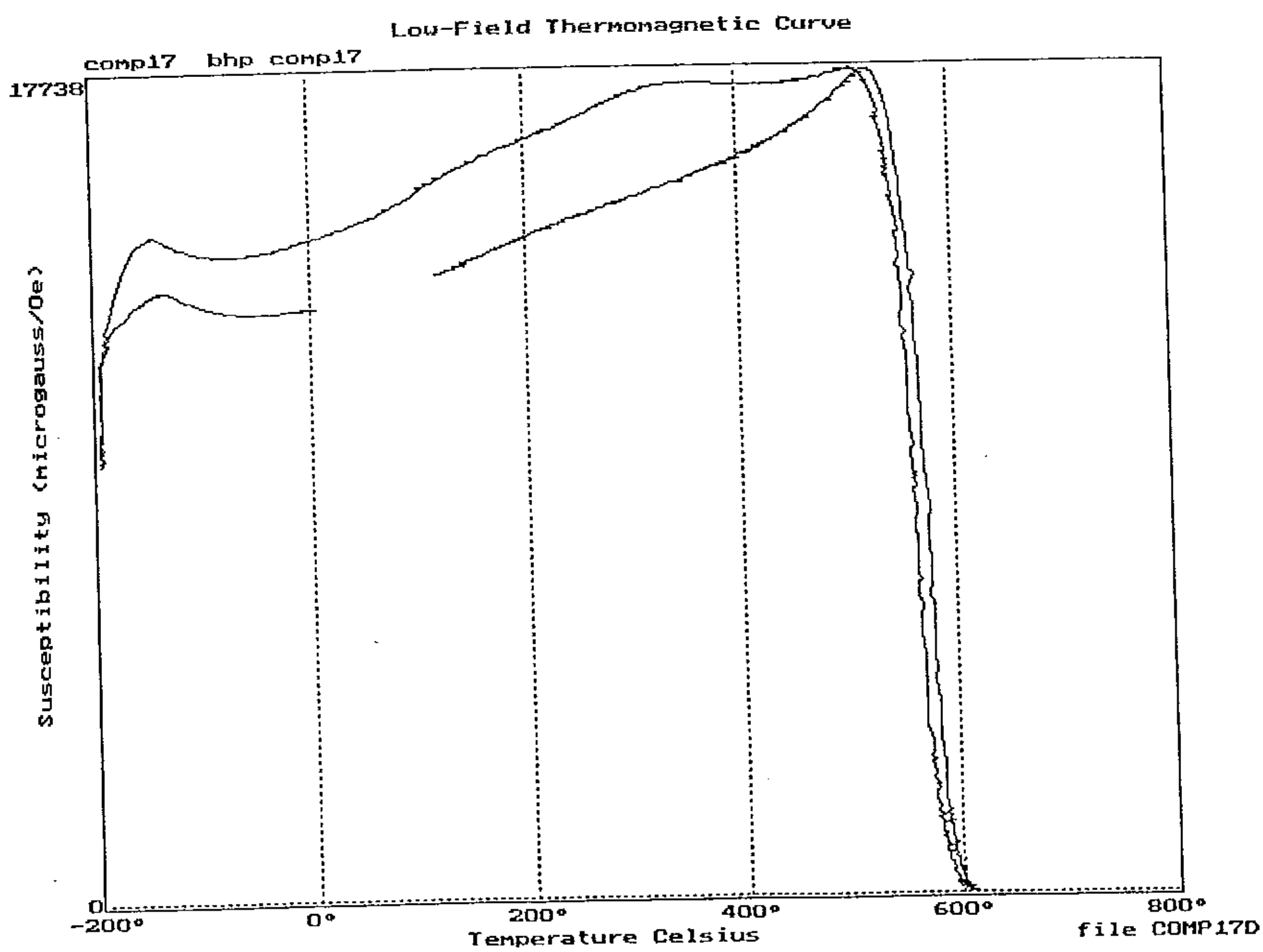
Low-Field Thermomagnetic Curve
comp17 bhp comp17
17738
0
Susceptibility (Microgauss/Oe)
-200°
0°
200°
400°
600°
800°
Temperature Celsius
file COMP17D

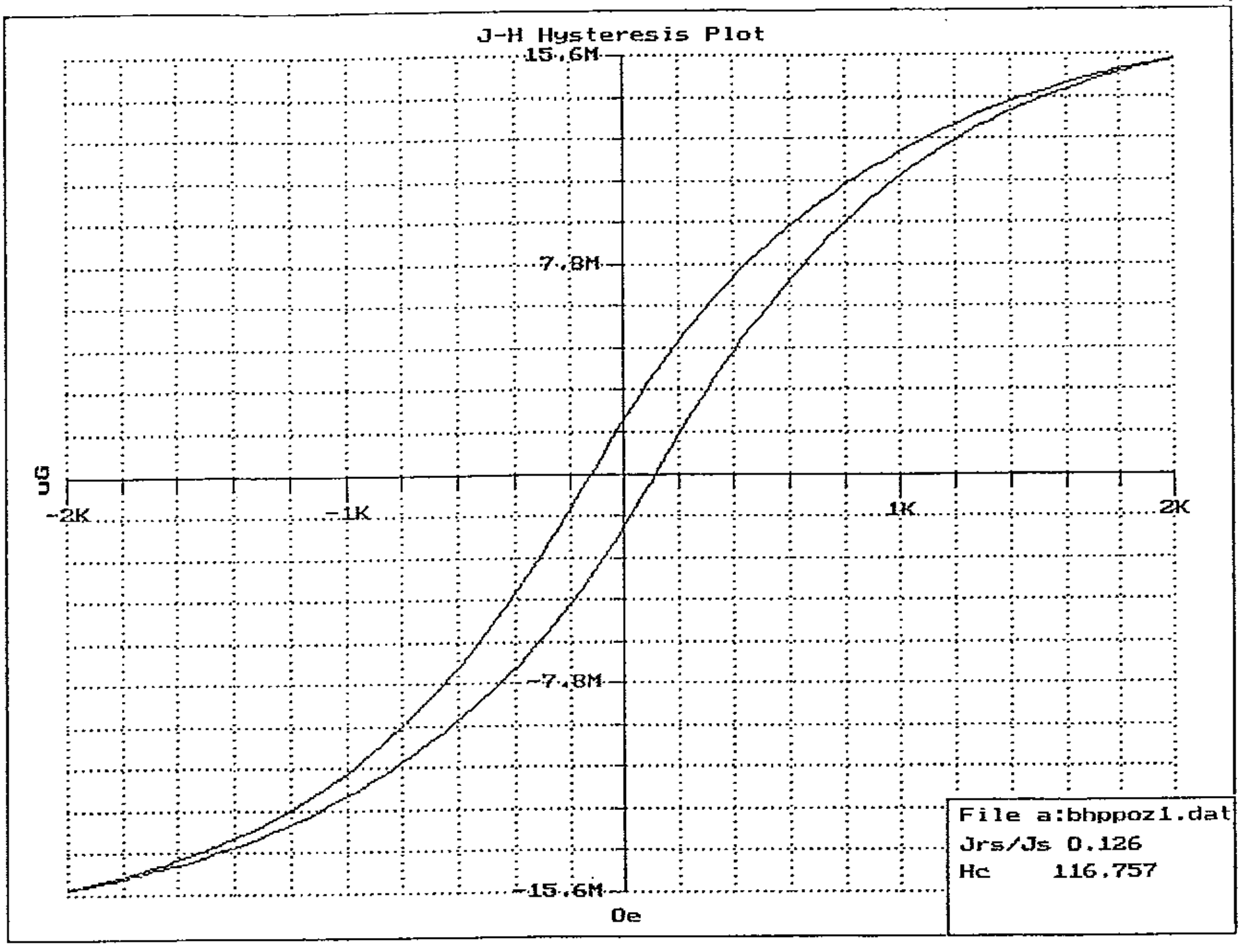
J-H Hysteresis Plot
15.6M
7.8M
-7.8M
-15.6M
uG
-2K
-1K
1K
2K
Oe
File a:bhppoz1.dat
Jrs/Js 0.126
Hc 116.757

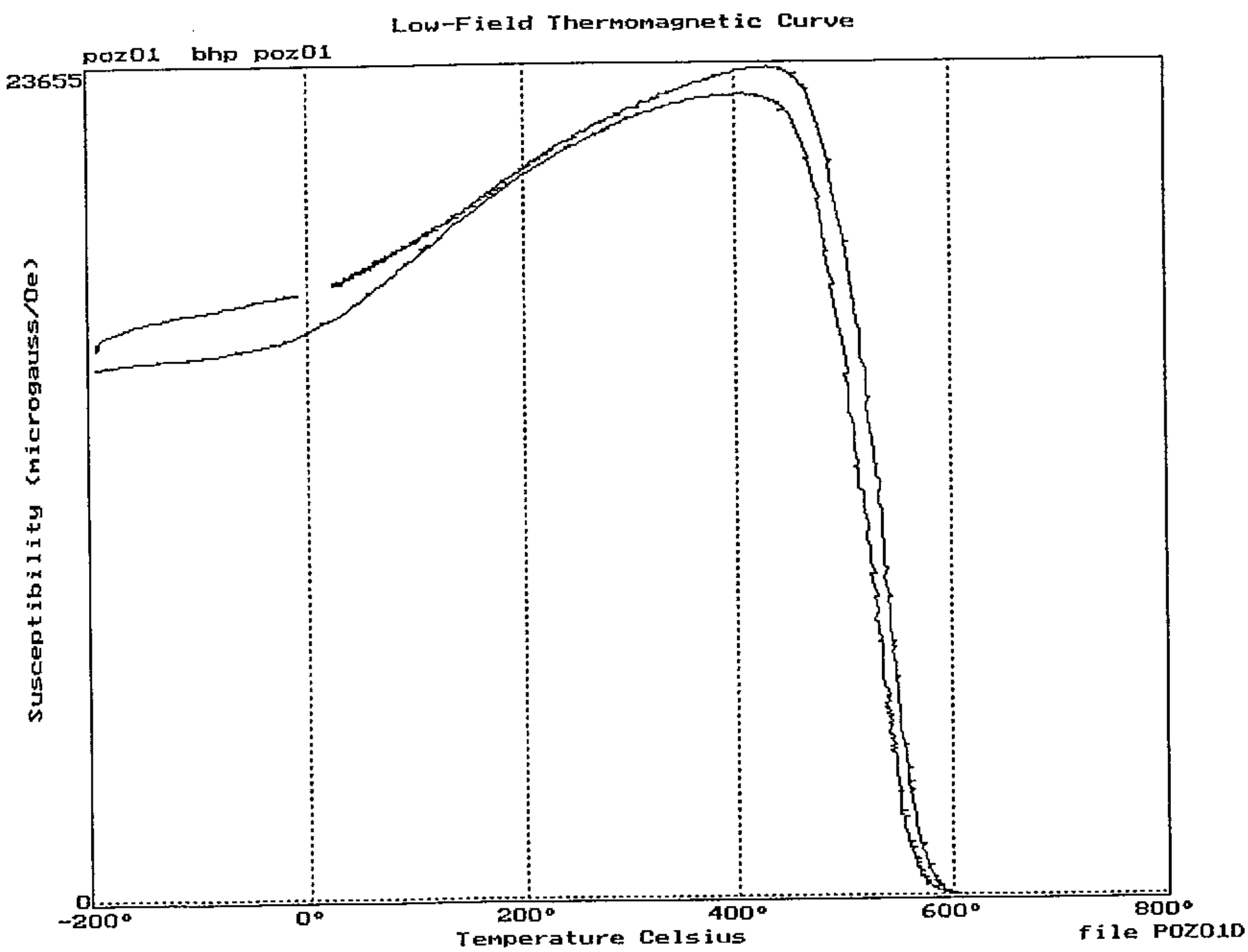
Low-Field Thermomagnetic Curve
poz01 bhp poz01
23655
0
Susceptibility (microgauss/Oe)
-200°
0°
200°
400°
600°
800°
Temperature Celsius
file POZ01D

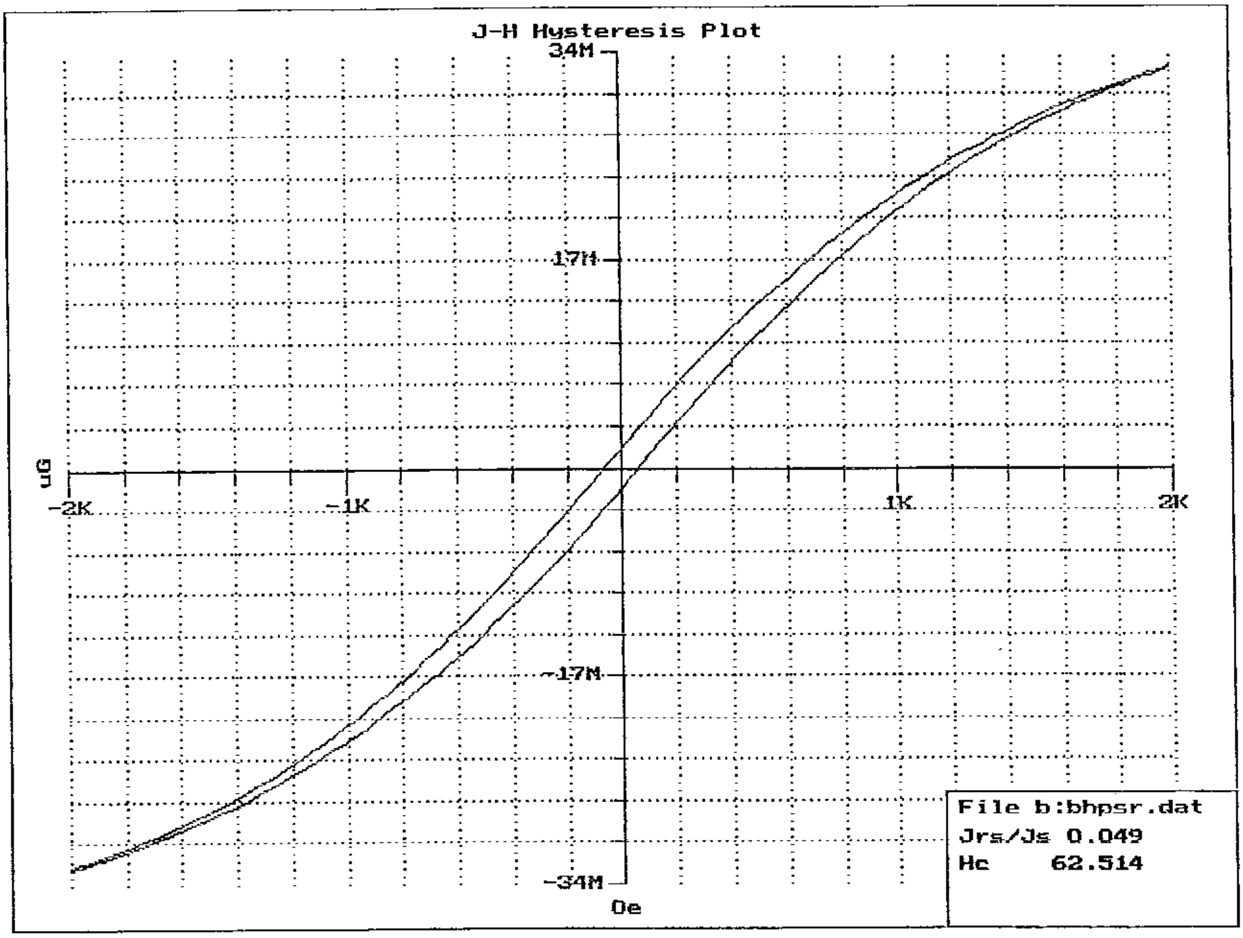
J-H Hysteresis Plot
34M
17M
-17M
-34M
uG
-2K
-1K
1K
2K
Oe
File b:bhpsr.dat
Jrs/Js 0.049
Hc 62.514

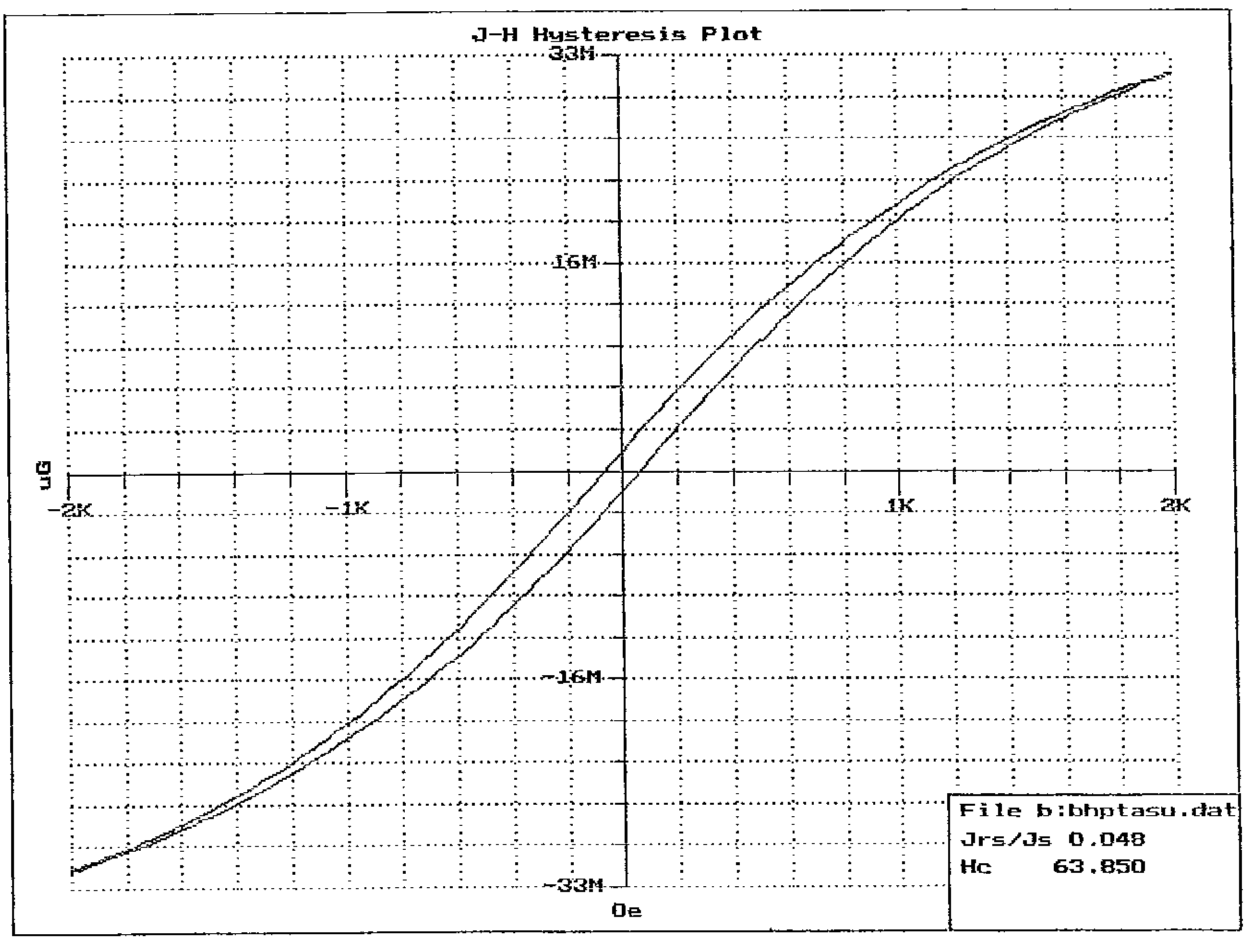
J-H Hysteresis Plot
33M
16M
-16M
-33M
uG
-2K
-1K
1K
2K
Oe
File b:bhptasu.dat
Jrs/Js 0.048
Hc 63.850